Please cite this article in press as: Shi et al., Electrochemical Synthesis of H_2O_2 by Two-Electron Water Oxidation Reaction, Chem (2020), https://doi.org/10.1016/j.chempr.2020.09.013

Chem

CellPress

Review

Electrochemical Synthesis of H_2O_2 by Two-Electron Water Oxidation Reaction

Xinjian Shi,[1,4] Seoin Back,[2,4] Thomas Mark Gill,[1,4] Samira Siahrostami,[3,*] and Xiaolin Zheng[1,*]

SUMMARY

Hydrogen peroxide (H_2O_2) is a high-value green chemical oxidant widely used for industrial bleaching, chemical synthesis, and disinfection. Industrially, H_2O_2 is produced through the energy-intensive anthraquinone process and distributed to the point of use. There is a growing interest in electrochemically producing H_2O_2 onsite to mitigate transportation cost and safety concerns and leveraging renewable electricity. Most research has been dedicated to the two-electron oxygen reduction to produce H_2O_2. For the past decade, growing attention has been paid to the two-electron water oxidation reaction (2e-WOR) to produce H_2O_2. This review focuses on the research progress on 2e-WOR, including basic principles, catalyst development, and H_2O_2 detection. Computational approaches to study candidate materials for 2e-WOR are detailed, and various experimental reports on catalysts are summarized. Ulterior electrochemical factors that impact H_2O_2 production are discussed, along with device-level design. Finally, a holistic perspective on water oxidation reaction is offered, and open questions for future work are presented.

INTRODUCTION

Hydrogen peroxide (H_2O_2) is a high-value green chemical oxidant widely used for chemical and medical applications both in industry and routine life. It is used for paper and fiber bleaching,[1] synthesis of other chemical species,[2] disinfection, and water treatment.[3]

Industrially, H_2O_2 is produced through the reduction/oxidation of anthraquinone.[4] Although this approach is efficient for large-scale production of H_2O_2, it requires large plants and infrastructure, and the H_2O_2 produced is crude, requiring costly extraction of solvents and reactants. Additionally, H_2O_2 is relatively unstable; hence, long-distance transportation presents substantial safety concerns. An alternative synthesis approach was devised to produce H_2O_2 from hydrogen (H_2) oxidation without organic reactants.[5] This approach has been well studied in laboratory environments and reaches some promising efficiencies with the proper catalysts.[6] However, this route necessitates harsh conditions, such as high temperatures and pressures, as well as the use of flammable H_2, both of which hinder its adoption.

Electrochemical routes provide an alternative means to produce H_2O_2 onsite. Though the use of electricity limits this route to small-scale development, this lends itself well to portable and distributed devices, which circumvent transportation safety concerns. Figure 1 shows three possible electrochemical devices for H_2O_2 production. Figure 1A shows a fuel cell that converts O_2 to H_2O_2, instead of H_2O, at the cathode via the two-electron O_2 reduction reaction (2e-ORR).[7] Figure 1B shows an electrolyzer that oxidizes

The Bigger Picture

Electrochemical synthesis of H_2O_2 represents a growing interest in the distributed production of valuable chemicals with renewable electricity, as evidenced by several recently published reviews on this topic. However, a review focusing exclusively on the electrochemical two-electron water oxidation reaction (2e-WOR) to produce H_2O_2 is still needed with tutorial styles to provide both theoretical and experimental fundamentals on this topic. Moreover, the related protocols and standardized metrics, which are crucially important for more consistent and reliable fundamental studies, are not well developed yet from the current reports. To fill in the gaps, our work discusses the current understanding and status of catalyst development for 2e-WOR from both theoretical and experimental perspectives. This review also outlines the questions to be answered for 2e-WOR and future research directions, including how to evolve H_2O_2 more efficiently and application development for accumulated H_2O_2.

Please cite this article in press as: Shi et al., Electrochemical Synthesis of H_2O_2 by Two-Electron Water Oxidation Reaction, Chem (2020), https://doi.org/10.1016/j.chempr.2020.09.013

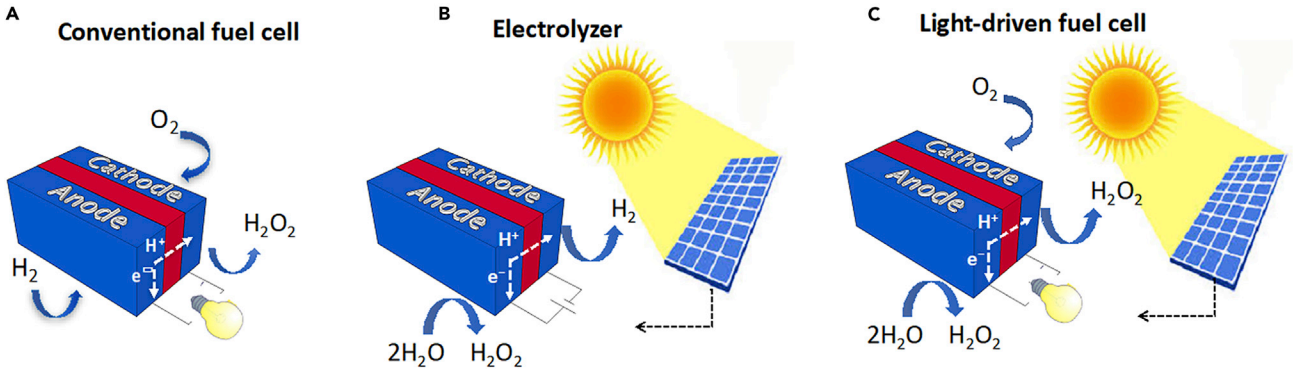

Figure 1. Three Possible Electrochemical Devices for H_2O_2 Production

(A) Fuel cell to produce H_2O_2 at the cathode via 2e-ORR.

(B) Electrolyzer for production of H_2O_2 at the anode via 2e-WOR.

(C) Light-driven fuel cell for two-sided production of H_2O_2 at the cathode via 2e-ORR and the anode via 2e-WOR.

H_2O to H_2O_2, instead of O_2, at the anode via the two-electron water oxidation reaction (2e-WOR). Figure 1C shows a light-driven fuel cell for two-sided production of H_2O_2 at the cathode via 2e-ORR and the anode via 2e-WOR.

Regardless of the device configuration, two reactions, i.e., 2e-ORR and 2e-WOR, are responsible for the electrochemical production of H_2O_2. The commonly studied electrochemical pathway to generate H_2O_2 is through the 2e-ORR.[8] 2e-ORR is an undesirable and competing reaction with the commonly studied four-electron ORR to produce water (H_2O) in fuel cells.[9,10] So far, several highly efficient electrocatalysts, such as alloys of Pt and Pd-Hg[11] and, most recently, carbon-based materials[12,13] have been developed for 2e-ORR,[14,15] and a few excellent reviews have been compiled for 2e-ORR.[16,17]

The 2e-WOR has also attracted increasing attention in recent years to produce H_2O_2. The 2e-WOR, in comparison with 2e-ORR, does not rely on the gas-phase reactant and provides a new approach for electrochemical H_2O_2 production. Figure 2 summarizes representative research on 2e-WOR chronologically. The top of the timeline focuses on experimental research and the bottom on theoretical research.[18] Initially, photocatalysis studies suggested the formation of H_2O_2 using wide-band-gap metal oxides such as TiO_2.[19,20] The first work on H_2O_2 production by 2e-WOR was reported in 2004, which uses a carbon-based catalyst in NaOH.[21] Since then, most research on 2e-WOR has focused on metal oxides.[22–27] In Theoretical Aspects for the Rational Design of 2e-WOR Catalysts, we first discuss the theoretical aspects of the rational design of 2e-WOR electrocatalysts, including different possible mechanisms, computational details for constructing the free energy diagram, and understanding trends of activity among different catalyst materials. We also discuss how catalyst stability can be estimated using computational material design. Lastly, we discuss the effects of solvation and density functional theory (DFT) functional choice on the energetics of reaction intermediates. Together, these theoretical frameworks provide important insights and guidance on the selection of 2e-WOR catalysts for experimental efforts.[28,29] In Experimental Methods for Characterizing 2e-WOR Catalysts we discuss experimental methods for characterizing 2e-WOR electrocatalysts, detail H_2O_2-quantification methods, and finally express our opinions on standardized reporting of electrocatalyst performance metrics. In Experimental Results of 2e-WOR Catalysts with Benchmarking Metrics, we summarize the most recent performance benchmarks of previously studied electrocatalysts.

[1]Department of Mechanical Engineering, Stanford University, Stanford, CA 94305, USA

[2]Department of Chemical and Biomolecular Engineering, Institute of Emergent Materials, Sogang University, Seoul, 04107, Republic of Korea

[3]Department of Chemistry, University of Calgary, Calgary, AB T2N 1N4, Canada

[4]These authors contributed equally

*Correspondence: samira.siahrostami@ucalgary.ca (S.S.), xlzheng@stanford.edu (X.Z.)

https://doi.org/10.1016/j.chempr.2020.09.013

Please cite this article in press as: Shi et al., Electrochemical Synthesis of H_2O_2 by Two-Electron Water Oxidation Reaction, Chem (2020), https://doi.org/10.1016/j.chempr.2020.09.013

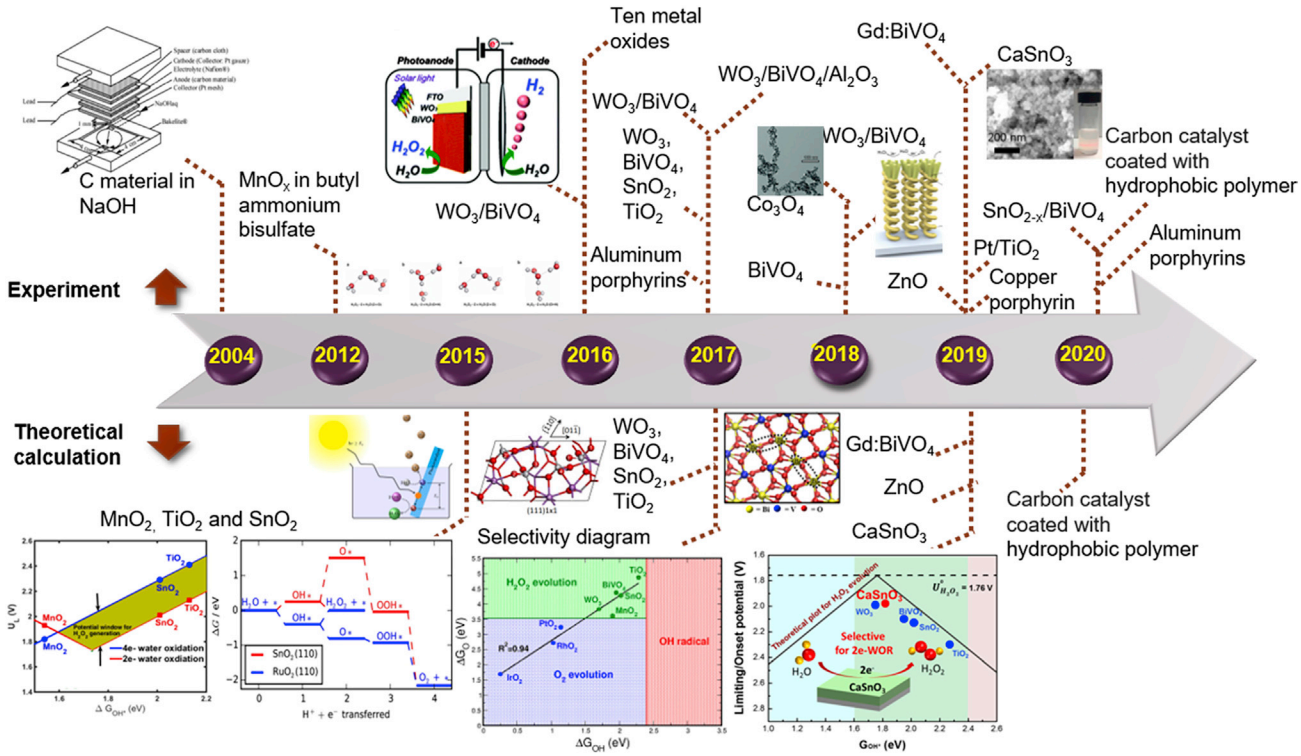

Figure 2. Previous Research on 2e-WOR for H_2O_2 Production Summarized Chronologically

The top part shows experimental works and the bottom part shows theoretical works. Each work is listed with its electrocatalysts for 2e-WOR. Reprinted with permission from Ando et al.[21] Copyright 2004 Elsevier. Reprinted with permission from Fuku et al.[22] Copyright 2016 Royal Society of Chemistry. Reprinted with permission from Fuku et al.[23] Copyright 2017 Royal Society of Chemistry. Reprinted with permission from Shi et al.[24] Copyright 2018 John Wiley & Sons, Inc. Reprinted with permission from Zhang et al.[26] Copyright 2018 Royal Society of Chemistry. Reprinted with permission from Shi et al.[28] Copyright 2017 Nature Publishing Group. Reprinted with permission from Mase et al.[30] Copyright 2016 Nature Publishing Group. Reprinted with permission from Park et al.[31] Copyright 2019 American Chemical Society. Reprinted with permission from Izgorodin et al.[32] Copyright 2012 Royal Society of Chemistry. Reprinted with permission from Baek et al.[33] Copyright 2019 American Chemical Society. Reprinted with permission from Shi et al.[25] Copyright 2018 Royal Society of Chemistry. Reprinted with permission from Kelly et al.[27] Copyright 2019 American Chemical Society. Reprinted with permission from Liu et al.[35] Copyright 2019 Royal Society of Chemistry. Reprinted with permission from Kuttassery et al.[36] Copyright 2017 John Wiley & Sons, Inc. Reprinted with permission from Kuttassery et al.[37] Copyright 2020 Royal Society of Chemistry.

We further discuss the other factors impacting 2e-WOR in Other Important Factors Affecting 2e-WOR to Produce H_2O_2 and provide future perspectives for the field in Summary and Outlook.

THEORETICAL ASPECTS FOR THE RATIONAL DESIGN OF 2E-WOR CATALYSTS

Three Possible Pathways for Electrochemical Water Oxidation Reaction

There are three possible pathways for electrochemical water oxidation reactions (WORs).[28,29] The reaction steps for the three WORs are schematically illustrated for a catalyst surface in Figure 3 and described in Equations 1, 2, and 3. The most studied WOR is the four-electron process (4e-WOR, Equation 1) used in electrolysis to produce O_2, which is commonly referred to as the oxygen evolution reaction (OER). Water oxidation can also proceed via a two-electron pathway to produce H_2O_2 (Equation 2) and a one-electron pathway to produce OH radicals ($OH^\bullet$, Equation 3). Notably, all three WORs start with the same first step, i.e., forming adsorbed OH (OH*). Both H_2O_2 and $OH^\bullet$ are of practical value due to their strong oxidizing abilities, and both can be used for sanitization and water disinfection. $OH^\bullet$ generally

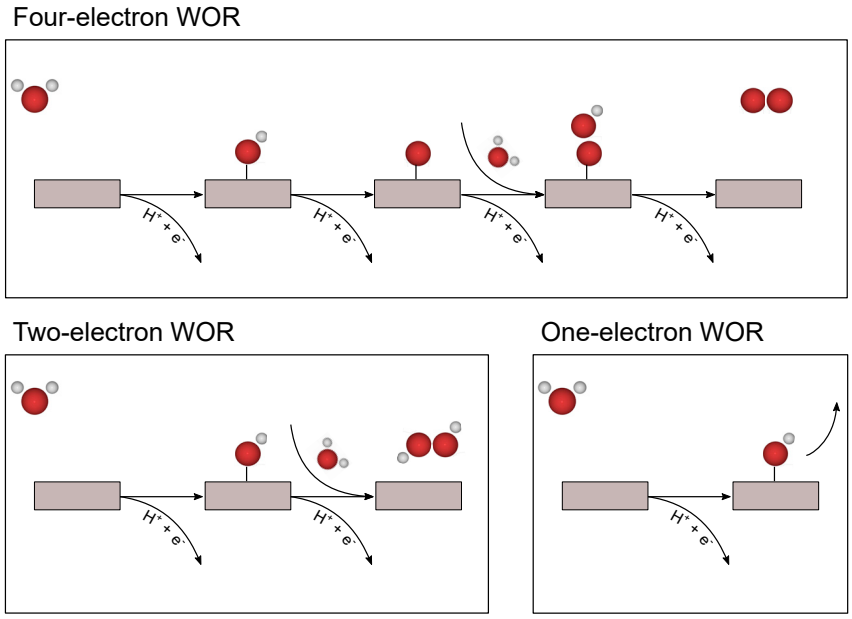

Figure 3. Schematics of Different Reaction Pathways for the Water Oxidation on a Catalytic Surface

has a short lifetime, so H_2O_2 is of more practical interest. Thermodynamically, 4e-WOR is the most favorable reaction, as it has the lowest equilibrium potential (E° = 1.23 V_{RHE}). Producing H_2O_2 from water (E° = 1.76 V_{RHE}) requires a 530 mV higher potential than producing O_2, making selective production of H_2O_2 intrinsically more challenging.

The 4e-WOR:

$$2H_2O \rightarrow O_2 + 4(H^+ + e^-) \quad (E^{\circ} = 1.23\ V_{RHE}) \qquad \text{(Equation 1)}$$

$$* + H_2O \rightarrow OH* + (H^+ + e^-) \qquad \text{(Equation 1A)}$$

$$OH* \rightarrow O* + (H^+ + e^-) \qquad \text{(Equation 1B)}$$

$$O* + H_2O \rightarrow OOH* + (H^+ + e^-) \qquad \text{(Equation 1C)}$$

$$OOH* \rightarrow * + O_2 + (H^+ + e^-) \qquad \text{(Equation 1D)}$$

The 2e-WOR:

$$2H_2O \rightarrow H_2O_2 + 2(H^+ + e^-) \quad (E^{\circ} = 1.76\ V_{RHE}) \qquad \text{(Equation 2)}$$

$$* + H_2O \rightarrow OH* + (H^+ + e^-) \qquad \text{(2A, the same as 1A)}$$

$$OH* + H_2O \rightarrow H_2O_2 + (H^+ + e^-) + * \qquad \text{(Equation 2B)}$$

The one-electron WOR (1e-WOR):

$$H_2O \rightarrow OH\bullet_{(aq)} + (H^+ + e^-) \quad (E^{\circ} = 2.38\ V_{RHE})^{38} \qquad \text{(Equation 3)}$$

Please cite this article in press as: Shi et al., Electrochemical Synthesis of H_2O_2 by Two-Electron Water Oxidation Reaction, Chem (2020), https://doi.org/10.1016/j.chempr.2020.09.013

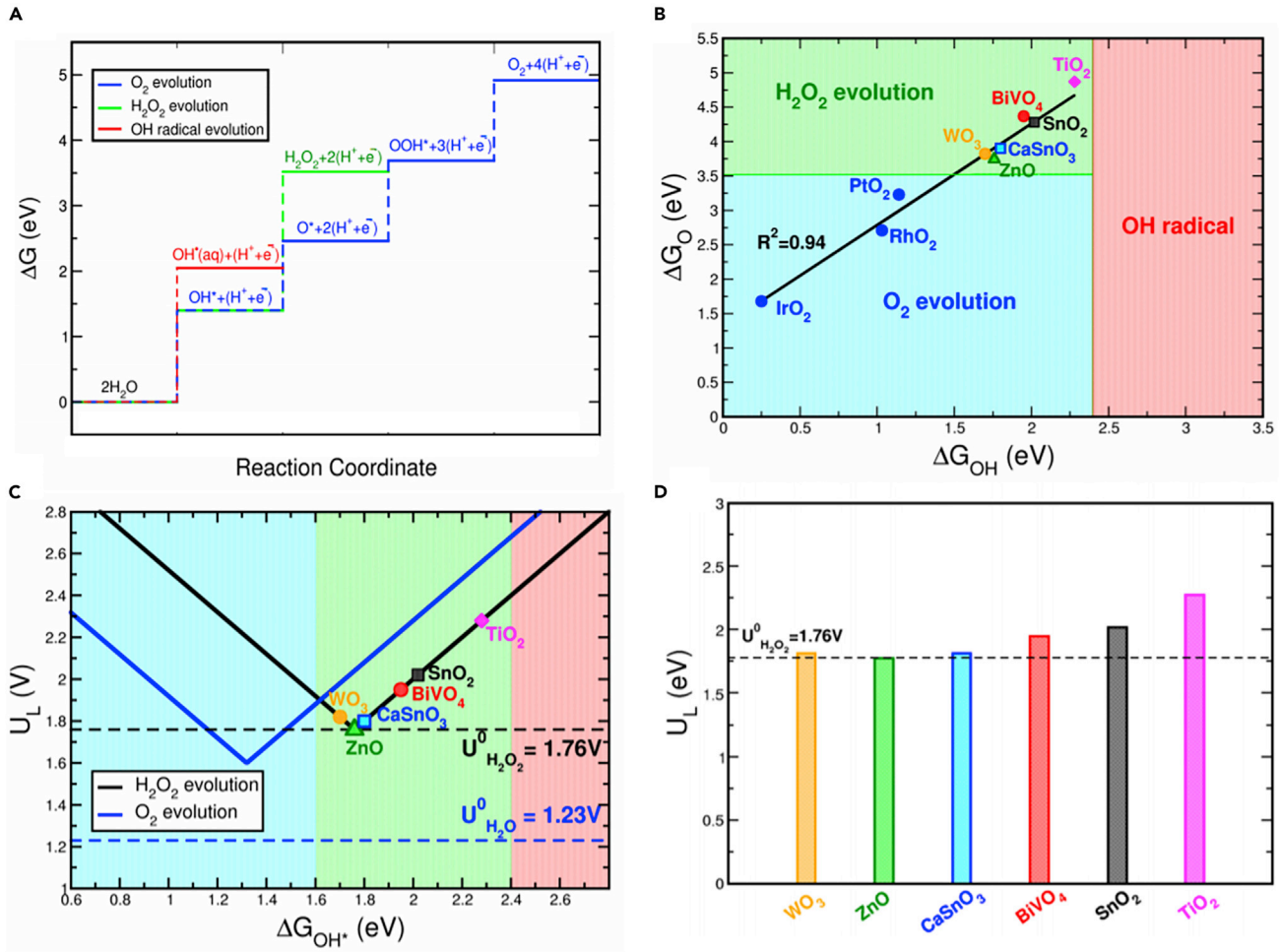

Figure 4. Summary of Calculation Results for Different Water Oxidation Pathways and Various Catalyst Species

(A) Free-energy diagram of three WOR pathways to OH• (red), H_2O_2 (green), and O_2 (blue) on a hypothetical ideal catalyst material at $U = 0$ V.

(B) Selectivity map among three WORs based on thermodynamic analysis of binding free energies of ΔG_{O*} and ΔG_{OH*}.

(C) Activity map for 2e- and 4e-WORs. The blue and black lines are the calculated limiting potential U_L for 2e- and 4e-WOR, respectively.

(D) DFT calculated U_L of 2e-WOR for several metal oxides. Reprinted with permission from Shi et al.[28] Copyright 2017 Nature Publishing Group. Reprinted with permission from Park et al.[31] Copyright 2019 American Chemical Society.

$$* + H_2O \rightarrow OH* + (H^+ + e^-) \qquad \text{(Equation 3A, the same as 1A)}$$

$$OH* \rightarrow OH\bullet_{(aq)} + * \qquad \text{(Equation 3B)}$$

Computational Details

To evaluate the energetics of WOR pathways, one needs to use DFT calculations to calculate the binding free energies of reaction intermediates, such as O*, OH*, and OOH* (ΔG_{O*}, ΔG_{OH*}, *and* ΔG_{OOH*}). The free energy of H_2 in the gas phase and H_2O in the liquid phase are used as the reference states. This is to avoid the explicit use of O_2 electronic energy due to the typical DFT error in describing triplet O_2 molecules.[39] Instead, standard reduction potential values are used, i.e., $\Delta G_{OH\bullet} = 2.38\ eV$, $\Delta G_{H_2O_2} = 2 \times 1.76\ eV$, and $\Delta G_{O_2} = 4 \times 1.23\ eV$ for the 1e−, 2e−, and 4e−WOR, respectively (Figure 4).

Please cite this article in press as: Shi et al., Electrochemical Synthesis of H_2O_2 by Two-Electron Water Oxidation Reaction, Chem (2020), https://doi.org/10.1016/j.chempr.2020.09.013

To incorporate the effect of the electrode potential on the free energy, the computational hydrogen electrode (CHE)[9] is used. The CHE sets the chemical potential of a proton-electron pair equivalent to that of gas-phase H_2 at potential U = 0 V, and when the potential U is applied, the chemical potential of an electron is shifted by $-eU$, where e and U are the elementary charge and electrode potential, respectively.

Free Energy Diagram of Three WOR Pathways

Figure 4A illustrates the use of free energy diagrams to capture the activity and selectivity of a hypothetical catalyst for the three WOR pathways. The first oxidation step, which is the same for the three WOR pathways, leads to adsorbed OH* species on the catalyst surface. If the OH*-binding free energy on the catalyst surface is weaker than the formation energy of aqueous hydroxyl radical, i.e., $\Delta G_{OH*} > 2.38\ eV$, it will be energetically favorable to release OH into the solution as $OH^{\bullet}$(1e-WOR). In contrast, if $\Delta G_{OH*} < 2.38\ eV$, the adsorbed OH* could be further oxidized to either H_2O_2 or adsorbed O* formation, depending on the ΔG_{O*}. Since the formation energy of H_2O_2, i.e., $\Delta G_{H_2O_2}$, in the solution is constant at 3.52 eV, catalyst materials with a weaker O*-binding free energy than $\Delta G_{H_2O_2}$, i.e., $\Delta G_{O*} > 3.52\ eV$, favor the formation of H_2O_2 (2e-WOR), while those stronger than 3.52 eV prefer the O_2 evolution pathway (4e-WOR). This thermodynamic analysis suggests that ΔG_{OH*} is the activity-determining factor, and ΔG_{O*} determines the selectivity between the three WOR products.[40] This analysis allows us to construct a selectivity map (Figure 4B) and rationalize product selectivity on many reported experimental catalysts for WORs.[29]

Linear Scaling Relations and Volcano Plot to Predict Catalytic Activities of 2e-WOR

Next, we determine the overpotentials ($\eta_{H_2O_2}$) and the limiting potentials (U_L) for 2e-WOR using scaling relations. DFT calculations of heterogeneous catalysis often observe linear scaling relations between binding energies of reaction intermediates that interact with surfaces through the same atomic species (e.g., N* with NH* and NH_2*, C* with CH*, CH_2*, and CH_3*).[41] These scaling relations have facilitated reducing the dimension of reaction networks, making it possible to predict catalytic activities for a large number of catalyst materials from simple binding-energy calculations rather than constructing full free energy diagrams.

For various oxide systems, scaling relations have been established between reaction intermediates; $\Delta G_{O*} = 2\Delta G_{OH*} + 0.28$ for metal-oxide surfaces[42] (solid line in Figure 4B) and $\Delta G_{OOH*} = \Delta G_{OH*} + 3.2$ eV.[42,43] By expressing ΔG_{O*} and ΔG_{OOH*} in terms of ΔG_{OH*}, we can express the limiting potentials (U_L) for the three WORs as a function of ΔG_{OH*}. For 4e-WOR, U_L has been expressed as $U_{L,O_2} = \max(\Delta G_{O*} - \Delta G_{OH*},\ 3.2\ eV - [\Delta G_{O*} - \Delta G_{OH*}])$ based on the scaling relation between ΔG_{OOH*} and ΔG_{OH*}.[42] This expression can be further simplified using the scaling relation between ΔG_{O*} and ΔG_{OH*} as follows: $U_{L,O_2} = \max(\Delta G_{OH*} + 0.28\ eV,\ 2.98\ eV - \Delta G_{OH*})$. For 1e-WOR and 2e-WOR, since OH* is the only reaction intermediate, the catalytic properties for both are solely determined by ΔG_{OH*}, as depicted by the solid black lines and the boundary between the green and red regions in Figure 4C. For 2e-WOR, the overpotentials ($\eta_{H_2O_2}$) and the limiting potentials (U_L) are determined based on ΔG_{OH*} (Equation 4A and Equation 4B) as follows:

$$U_{L,H_2O_2} = [\max(\Delta G_{OH*},\ 1.76\ eV - \Delta G_{OH*})]/e \quad \text{(Equation 4A)}$$

$$\eta_{H_2O_2} = U_{L,H_2O_2} - 1.76\ eV \quad \text{(Equation 4B)}$$

Please cite this article in press as: Shi et al., Electrochemical Synthesis of H_2O_2 by Two-Electron Water Oxidation Reaction, Chem (2020), https://doi.org/10.1016/j.chempr.2020.09.013

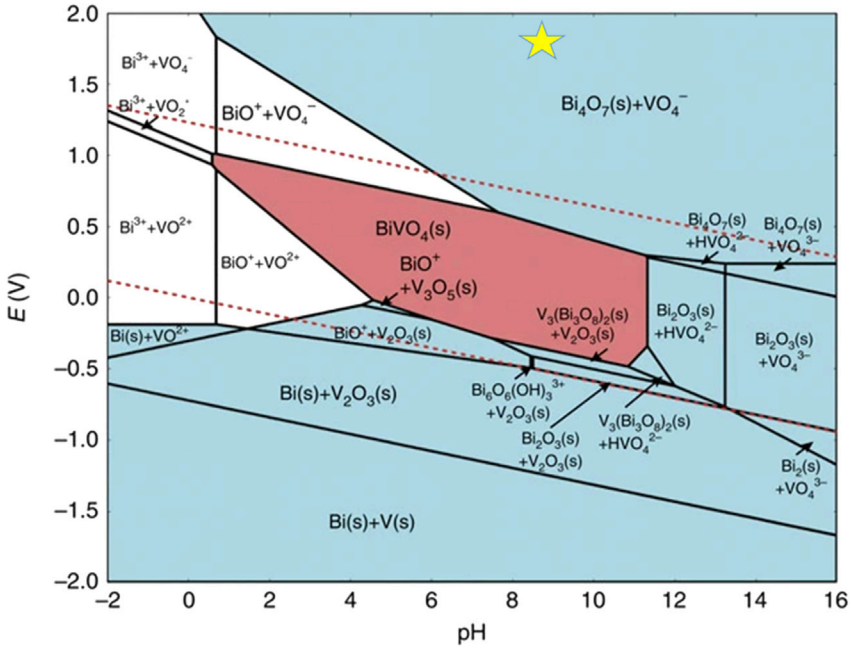

Figure 5. The Materials Project Pourbaix Diagram of 50%–50% Bi-V System in Aqueous Solution, Assuming a Bi-Ion Concentration of 10^{-5} mol/kg and V-Ion Concentration of 10^{-5} mol/kg

The upper and lower dashed lines correspond to the equilibrium potentials for the OER and HER, respectively. The blue regions denote stable solid compounds, while the pink region denotes the pH and potential window in which $BiVO_4$ is stable. The yellow star denotes the experimental conditions for 2e-WOR in 2M $KHCO_3$, a typical electrolyte for 2e-WOR. Reprinted with permission from Toma et al.[46] Copyright 2016 Nature Publishing Group.

Figure 4C shows the volcano plots of U_{L,H_2O_2} and U_{L,O_2} as a function of ΔG_{OH*}. When $U_{L,H_2O_2} < U_{L,O_2}$, 4e-WOR is thermodynamically favored over 2e-WOR. The middle section of Figure 4C is the preferred range for 2e-WOR, where the OH* binds to the catalyst surface neither too strongly nor too weakly (1.6 to 2.4 eV). The optimum ΔG_{OH*} is close to 1.76 eV. Using this approach, we have calculated the U_{L,H_2O_2} for various oxide materials as shown in Figure 4D. These DFT predictions were validated by experimental results as discussed in the section "Activity and Selectivity of Various Catalysts toward 2e-WOR".

Predicting the Stability of Electrocatalysts under 2e-WOR Conditions

The reaction conditions of 2e-WOR expose catalysts to high oxidation potentials over 1.76 V versus reversible hydrogen electrode (RHE), so the electrochemical stability of catalysts is a critical factor for H_2O_2 production. The Pourbaix diagram can be generated by using Pymatgen[44] and Materials Project[45] and is a great thermodynamic tool to predict the electrochemical stability of catalysts. For example, Figure 5 shows a hybrid computational and experimental Bi-V Pourbaix diagram, which shows that $BiVO_4$ is only stable[46] in the low potential range of 0.3 ~ 1.1 V_{RHE} in the pH range (~8.3) of bicarbonate-based electrolytes often used in 2e-WOR studies, while vanadium oxides (VO_4^-) dissolve at higher potentials. Indeed, $BiVO_4$ shows poor electrochemical stability as reported by Toma et al. (Figure 5)[46] even though it has good catalytic activity for 2e-WOR. We note that the Pourbaix diagram only accounts for the thermodynamic stability, not kinetics. Nevertheless, the Pourbaix diagram, together with the descriptors discussed in Computational Details, should be used to identify both active and stable electrocatalysts for 2e-WOR for further experimental studies.

Please cite this article in press as: Shi et al., Electrochemical Synthesis of H_2O_2 by Two-Electron Water Oxidation Reaction, Chem (2020), https://doi.org/10.1016/j.chempr.2020.09.013

Accuracy and Limitations of DFT Analysis

Choice of the Exchange-Correlation Functional

The accuracy of DFT calculations for catalytic activities is critically affected by the choice of the exchange-correlation functional. Due to the high oxidation potential required for 2e-WOR (>1.76 V_{RHE}), metal oxides may be the only materials that are somewhat stable catalysts for this reaction, which has led to their widespread use. However, the electronic and thermodynamic properties of bulk metal oxides are known to be overestimated by the standard exchange-correlation functionals, such as generalized gradient approximation (GGA) or local density approximation (LDA).[47] The overestimation is due to a self-interaction error of localized *d*- and *f*-electrons. To solve this problem, the Hubbard *U* correction[48] is generally used to treat the strong onsite Coulomb interaction in oxides. However, it is not trivial to determine the Hubbard *U* values, which often need to be benchmarked against experimental data. Cococcioni and Gironcoli suggested that the Hubbard *U* values can be calculated via a linear-response method.[49] Hu et al. applied this method[50] on various rutile metal oxides for 4e-WOR and found that applying *U* correction shifts the adsorption energies endothermically but does not significantly affect the general trend established without *U* correction, such as scaling relations of binding energies. Overall, applying *U* correction improves the agreement between the calculated limiting potential and the experimental onset potential.

Though the GGA functionals are not accurate for calculating the band gap and bulk properties of metal oxides, they have predicted chemisorption[51] properties with great accuracy. The DFT calculated values for adsorption energies are typically found to be within $\pm$0.2 eV of experimental results, depending on the specific GGA functional used.[51] These results explain why it is still useful to use GGA functionals for predicting binding energies. Another example is a report by Chuasiripattana et al., which shows CO binding energy on the ZnO (0001) surface using the PBE functional is in agreement with experiments.[52] Also, a microkinetic study using BEEF-vdW qualitatively predicted experimentally observed methanol synthesis rates,[53] implying that the GGA functional describes surface chemical properties of oxides with reasonable accuracy. Among different existing GGA functionals, we often use RPBE (revised Perdew-Burke-Ernzerhof) for predicting trends in 2e-WOR, which has proven to be very successful and in very good agreement with experiments.[27–29,31,54]

Solvation Effect

DFT calculations for electrocatalysis need to accurately account for the effect of water on the adsorption energies of reaction intermediates. Water structure and its effect on the adsorption energies of reaction intermediates have been investigated for several close-packed metal surfaces using hexagonal water bilayer structures,[55] and it was found to be significant for the energetics of ORR.[56] However, Casalongue et al. found that the solvation effect decreases as the potential increases.[57] On the other hand, the effect of water solvation on other catalyst surfaces, such as oxides, was unknown, as it is difficult to obtain accurate water structures due to the dynamic behavior of water molecules near the catalyst surfaces. Siahrostami and Vojvodic[58] explicitly studied the effect of water networks on three different rutile oxides (IrO_2, RuO_2, and TiO_2 (110)) for 4e-WOR. They found that water molecules adsorb strongly at available metal sites on the surface of rutile oxides (Figure 6), and this chemical interaction becomes weaker as more water molecules are introduced. Interestingly, water forms well-defined chains with adjacent water molecules on all three studied rutile surfaces, resembling the bulk water network as the water coverage increased to 2.0 ML. The presence of the water layers has little impact on the predicted catalytic activities (the limiting potentials) for 4e-WOR, although the water layer stabilizes

Please cite this article in press as: Shi et al., Electrochemical Synthesis of H_2O_2 by Two-Electron Water Oxidation Reaction, Chem (2020), https://doi.org/10.1016/j.chempr.2020.09.013

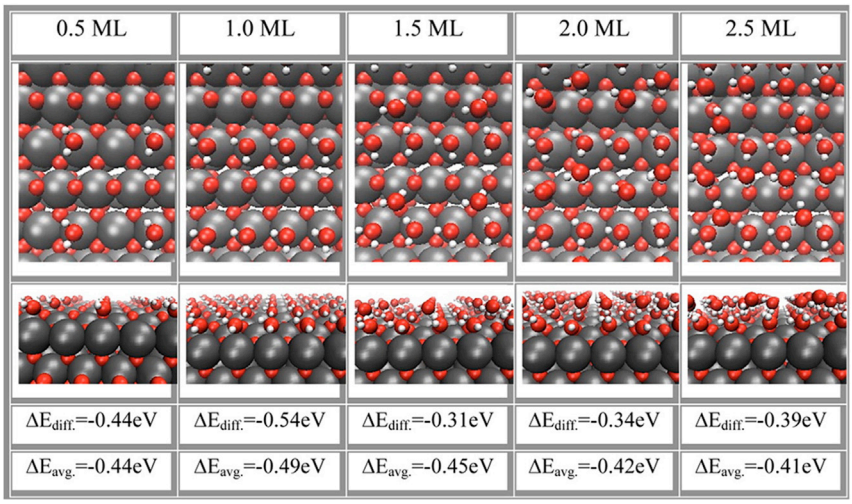

Figure 6. Top and Side Views of the Most Stable Configuration for Different Water Coverages on the Defect-free TiO_2 (110) Surface

Differential and average adsorption energies are given in the last rows. Titanium, oxygen, and hydrogen atoms are represented by dark gray, red, and white spheres. The surface is repeated several times in both the [100] and [010] directions. Reprinted with permission from Siahrostami et al.[58] Copyright 2015 American Chemical Society.

the individual intermediates through hydrogen-bonding interactions. For 2e-WOR, OH* is the sole intermediate and descriptor of the activity. Therefore, adding a 0.15eV correction for the water solvation effect is necessary. Nevertheless, given that high potential weakens the water solvation effect and the inclusion of water layers does not affect the overall trends of the predicted catalytic activity and selectivity, we conclude that common DFT methods are sufficiently accurate for WORs without solvation corrections.

As a brief conclusion, DFT analysis is a powerful tool for predicting the catalyst activity, selectivity, and stability of the electrocatalyst for 2e-WOR. ΔG_{OH*} was found to be the descriptor for the activity and selectivity of WOR in general. The calculated results match well with many experimental data so far.

EXPERIMENTAL METHODS FOR CHARACTERIZING 2E-WOR CATALYSTS

Protocols for Measuring Activity, Selectivity, and Stability of 2e-WOR Catalysts

Experimental methods for evaluating 4e-WOR catalysts for O_2 evolution are well established in the literature, and substantial efforts have been made to benchmark catalyst performance.[59] As a nascent field, 2e-WOR catalysis demands similar standardization in both measurement and reporting protocols to ensure continued progress. In electrocatalytic studies, three general aspects describe material performance: activity, selectivity, and stability. Activity is defined by the reduction of the activation energy barrier for the desired reaction, selectivity is the specificity of the reaction toward the desired product (H_2O_2 in the case of 2e-WOR), and stability is the amount of time the catalyst can carry out the desired reaction without substantial degradation in the other two performance metrics.

Electrocatalytic activity in 2e-WOR is measured by either linear-sweep voltammetry (LSV) or cyclic voltammetry (CV). These experiments allow for the determination of

Please cite this article in press as: Shi et al., Electrochemical Synthesis of H_2O_2 by Two-Electron Water Oxidation Reaction, Chem (2020), https://doi.org/10.1016/j.chempr.2020.09.013

the overpotential $\eta_{H_2O_2}$ (Equation 4B) defined as the voltage beyond the thermodynamic limit (1.76 V versus RHE in the case of H_2O_2) needed to achieve a given current density. The overpotential should be measured carefully to compare the activity of catalysts between labs. First, the current density being measured should be purely faradic and attributable to H_2O_2 generation only. Accordingly, before overpotential measurement, cyclic voltammograms should be run between the non-faradic region and potentials more than the maximum voltage in the LSV until the change in the characteristic between one cycle and the next is negligible. Sometimes called "activation cycling,"[60] this process ensures that the electrocatalyst is oxidized to its *in operando* state before overpotential determination. This step is particularly important for 2e-WOR as the high anodic bias necessary to generate H_2O_2 is sufficient to oxidize nearly all transition metals,[61] meaning that the initial LSV likely includes current contributions from the oxidation of the catalyst. Furthermore, non-faradic contributions can become appreciable when scan rates in LSV exceed 50 mV/s.[59] In this instance, some of the observed currents are attributable to double-layer charging, rather than H_2O_2 generation. Accordingly, voltammograms used to determine the overpotential should be obtained with low sweep rates, and supplementary LSVs should be provided showing that the characteristics are independent of the sweep rate. Finally, all LSVs should be iR-corrected for the uncompensated resistance of the electrochemical cell to remove solution and ulterior circuitry resistances.

Catalyst selectivity toward H_2O_2 can either be measured *in situ* (to be discussed in Quantification Methods for H_2O_2) or via an accumulation-based approach. For accumulation-based methods, selectivity is typically measured using chronoamperometry (CA) via the application of a constant bias above the onset potential. The amount of H_2O_2 produced is then measured by some external means (see Quantification Methods for H_2O_2). The figure of merit describing the selectivity in accumulation-based studies is the faradic efficiency (FE_{2e-WOR}), defined as the ratio between the amount of generated H_2O_2 and the theoretically generated H_2O_2 based on the measured current and perfect assumed efficiency:

$$FE_{2e-WOR}(V_{app},\ t) = \frac{\text{Amount of generated } H_2O_2}{\text{theoretically generated } H_2O_2} \times 100 = \frac{M_{H_2O_2}}{\frac{\int_0^t I(t)dt}{nF}} \times 100 \quad \text{(Equation E1)}$$

where $M_{H_2O_2}$ is the molar amount of generated H_2O_2 (moles); $I(t)$ is the measured current as a function of time under the given applied bias (A); t is the duration over which the measured H_2O_2 is accumulated (s); n is 2 as two electrons are needed to form one molecule of H_2O_2; F is Faraday's constant (96,485 C/mol). Note that *E1* results in FE_{2e-WOR}expressed as a percentage. Due to its sensitivity to the applied bias, the FE_{2e-WOR} needs to be evaluated at various potentials, typically in the range of 1.8–3.0 V versus RHE.

Though the methodology for calculating FE_{2e-WOR} is straightforward, the determination of $M_{H_2O_2}$ is difficult due to the poor stability of H_2O_2 in electrochemical environments. H_2O_2 can be further reduced to H_2O (reverse reaction of reaction Equation 3), oxidized to O_2, or undergo disproportionation to form H_2O and O_2, both homogeneously in the electrolyte and heterogeneously on electrodes. These processes are affected by the electrolyte species and purity,[22] pH,[22,62] catalysts,[27,28] and the concentration of H_2O_2 (see Other Important Factors Affecting 2e-WOR to Produce H_2O_2).[62] In addition, H_2O_2 accumulates in the electrolyte, which may impact the selectivity by affecting the equilibrium of the electrochemical environment. Several measures should be taken during the electrochemical generation of

Please cite this article in press as: Shi et al., Electrochemical Synthesis of H_2O_2 by Two-Electron Water Oxidation Reaction, Chem (2020), https://doi.org/10.1016/j.chempr.2020.09.013

H_2O_2 to improve the accuracy of the selectivity determination. First, the electrolyte should be vigorously circulated by stirring or pumping during the CA test. This prevents H_2O_2 concentration gradients from forming within the electrochemical cell, thereby reducing the impact of H_2O_2 accumulation on local equilibrium and improving the accuracy of the accumulation-based H_2O_2-quantification methods. If possible, the anode and cathode should also be placed in separate compartments to prevent H_2O_2 degradation by cathodic materials. Finally, it is recommended that when measuring the accumulated H_2O_2, aliquot volumes over 20% of the total electrolyte volume in the cell are extracted to minimize the impact of any remaining concentration gradients.

Catalyst stability is evaluated using either CA or chronopotentiometric (CP) methods. A constant potential (CA) or current (CP) is applied, while the other variable is measured. Interestingly, no well-defined figure of merit exists to describe catalyst stability in water-oxidation studies. Generally, a stable catalyst in 2e-WOR will exhibit a steady current under a constant applied bias for several hours to several days. During longer measurements, electrolytes should be stirred and changed periodically to maintain a constant volume and to prevent excess H_2O_2 accumulation from inhibiting further production.

Quantification Methods for H_2O_2

Accurate measurement of H_2O_2 concentration in aqueous electrolytes is critical in evaluating the selectivity of electrocatalysts for 2e-WOR. Generally, methods, including colorimetric test strips,[15,33] titration,[63] spectrophotometry,[64] chemiluminescence,[65] and fluorescence,[66] have been used to measure aqueous concentrations of H_2O_2. For electrochemically generated H_2O_2, methods can be separated into *in situ* and accumulation-based measurements. *In-situ* measurements determine selectivity toward H_2O_2 during the water-oxidation process, whereas accumulation-based methods rely on measuring the concentration of H_2O_2 in the cell after water oxidation has occurred for a prolonged period (typically several minutes). Each method offers unique advantages that may be leveraged depending on the application. Broadly, *in situ* methods offer the advantage of circumventing the issue of H_2O_2 degradation during prolonged measurement while accumulation-based approaches more accurately reflect generated H_2O_2 amounts that would be observed in a static electrolyzer system. Using rotating ring-disk electrodes (RRDE) is the method of choice for *in situ* studies, whereas titration,[34] spectrophotometry,[26,68] and colorimetric test strips[28,31] are all commonly employed to measure accumulated H_2O_2 that has been generated electrochemically.

In RRDE experiments, two concentric electrodes are placed on a cylindrical shaft (Figure 7A). The disk electrode is held at a fixed applied bias suitable for 2e-WOR or swept linearly through the 2e-WOR region, while the ring electrode is held at sufficient bias for selective H_2O_2 oxidation to O_2. Both reactions typically exhibit high overpotentials, necessitating applied potentials several hundred millivolts higher than their respective thermodynamic limits. Rotation of the shaft induces laminar electrolyte flow from the inner disk electrode, where oxidation of water occurs (i.e., H_2O to H_2O_2 and O_2), to the outer ring electrode, where selective oxidation of the generated peroxide occurs (i.e., H_2O_2 to O_2).[69] The currents observed at the two electrodes can be used to determine the molar ratio of produced H_2O_2[70]:

$$X_{2e-WOR,\ RRDE} = 200\% \times \frac{\left|i_{ring}\right| / N_{H2O2}}{\frac{\left|i_{ring}\right|}{N_{H2O2}} + \left|i_{disk}\right|} \qquad \text{(Equation E2)}$$

Please cite this article in press as: Shi et al., Electrochemical Synthesis of H_2O_2 by Two-Electron Water Oxidation Reaction, Chem (2020), https://doi.org/10.1016/j.chempr.2020.09.013

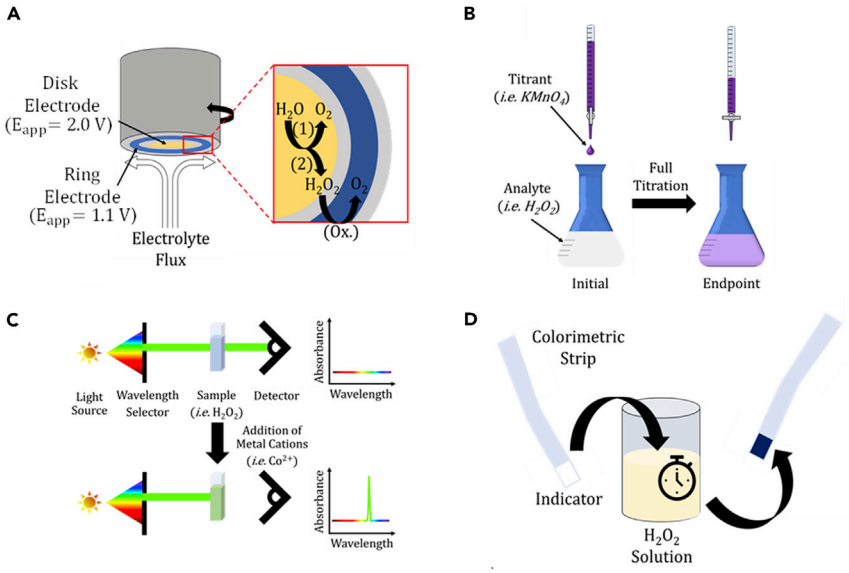

Figure 7. Schematic Representations of *In Situ* and Accumulation-based Hydrogen Peroxide Quantification Methods

It includes rotating ring disk electrode (A), titration method (B), UV-vis spectroscopy (C), and colorimetric strips (D). Reprinted with permission from Gill et al.[80] Copyright 2020 American Chemical Society.

where i_{ring} is the measured ring current, N_{H2O2} is the H_2O_2 collection efficiency, i_{disk} is the measured disk current, and $X_{2e-WOR,\ RRDE}$ is expressed as a percentage. Note that this equation has primarily been applied in 2e-ORR studies,[13] but the derivation for 2e-WOR results in the same equation, assuming OH• generation is negligible. The detection limit of this method depends on the minimum measurable current at the ring and the percentage of product evolved at the disk, which is transported to the ring (i.e., the collection efficiency).[71] Notably, Zhou et al. recently demonstrated that accurate RRDE experiments require calibrating the collection efficiency and proving that the current at the ring is mass-transfer limited in the chosen electrolyte.[72] Accordingly, these two steps should be taken prior to *in situ* measurements by RRDE. Furthermore, verification should be provided that the ring electrode is selective toward oxidation of H_2O_2 before Equation E2 can be used for accurate quantification. The distinct advantage of using RRDE to measure H_2O_2 is that it is not impacted by the instability of H_2O_2 in aqueous solutions; transit time between the disk and ring electrodes is typically very small, such that significant degradation of H_2O_2 should not occur between the generation and measurement steps.

Here, we pause to clarify H_2O_2 selectivity reporting in RRDE studies present in the literature. Xia et al. recently articulated the differences between reporting $X_{2e-WOR,\ RRDE}$ and faradaic efficiency ($FE_{2e-WOR,RRDE}$) as the primary H_2O_2 selectivity metric in RRDE studies:[73]

$$FE_{2e-WOR,RRDE} = 100\% * \frac{|i_{ring}|}{N_{H2O2}} \Big/ |i_{disk}| \qquad \text{(Eqaution 3)}$$

They argue that the validity of *E*2 is impacted by side reactions, while *E*3 is more relevant to operational costs in electrolyzers and could more easily standardize comparisons between 2e-ORR and 2e-WOR. For these reasons, the authors suggest that $FE_{2e-WOR,RRDE}$ should be used as the primary H_2O_2-selectivity-reporting metric in

Please cite this article in press as: Shi et al., Electrochemical Synthesis of H_2O_2 by Two-Electron Water Oxidation Reaction, Chem (2020), https://doi.org/10.1016/j.chempr.2020.09.013

RRDE studies, with which we wholly agree, provided the ring reaction is proven to be selective toward H_2O_2 detection.

Titration-based methods are employed by the dropwise addition of titrant to the H_2O_2-containing solution (Figure 7B). Leveraging the redox properties of H_2O_2, the titrant is either reduced or oxidized by the H_2O_2, resulting in a color change of the titrant. When the analyte solution assumes the color of the titrant, it indicates that all the H_2O_2 has reacted and thus the endpoint has been reached. Assuming that the reaction between titrant and H_2O_2 is stoichiometric, the initial molar amount of H_2O_2 in the solution can be calculated. Many titrants have been developed and used in electrochemical H_2O_2 studies, including $KMnO_4$-,[34] $Ce(SO_4)_2$,[15] and Ti-based assays, [30,74]among others.[75] The minimum detection limit of titration methods is 1,000–10,000 ppm H_2O_2 (0.1–1 wt %),[76] though recent work has reduced the titrant concentration to allow determination of more dilute H_2O_2 solutions.[73] Titration provides substantial advantages over other methods listed herein as it requires no calibration or specialized equipment. However, though diluting the titrant allows for the detection of H_2O_2 at lower concentrations it also introduces greater ambiguity in endpoint determination, likely reducing accuracy and reproducibility. The accuracy of titration-based methods for measuring accumulated H_2O_2 at concentrations below 1,000 ppm demands further study.

Spectrophotometric measurement of H_2O_2 relates the ultraviolet and visible (UV-vis) light absorbance of an aqueous solution at specified wavelengths to the concentration of H_2O_2 in the solution. Mechanistically, a transition-metal ion is oxidized or reduced upon addition of H_2O_2, resulting in a color change (Figure 7C). The magnitude of the absorbance at the wavelength corresponding to the developed color is linearly related to the initial concentration of H_2O_2. To quantify the accumulated H_2O_2, this linear relationship must be established by careful calibration using known concentrations of H_2O_2. Spectrophotometric assays commonly employed for H_2O_2 measurement include Fe based,[68] Cu based,[77] and cobalt-carbonate.[78] Minimum detection limits for these methods range from 0.3 to 4 ppm.[79] Because spectrophotometric quantification relies on calibration, the accuracy of the method is inherently dependent on the accuracy of the "known" H_2O_2 concentration of the samples used for calibration. Furthermore, the temporal stability of the color change is often debated, suggesting a possible source of error. Assuming accurate calibration, the lower minimum detection limit and purely quantitative nature of spectrophotometric methods make them strongly preferred over titration-based approaches.

Colorimetric strips are used by immersing a commercially available indicator in the H_2O_2-containing solution. Given sufficient time, the H_2O_2 reacts with a chemical in the indicator, resulting in a color change (Figure 7D). Unfortunately, the nature of these indicators is largely proprietary. The minimum detection limit of colorimetric strips varies by manufacturer, ranging from 0.5 to 1,000 s of ppm of H_2O_2. Strips offer uniquely facile H_2O_2 measurement but suffer from time sensitivity, interference effects, and relatively poor accuracy (often $\pm$20%, according to the manufacturer of Quantofix®). In accumulation-based studies, colorimetric strips should be used to verify the presence of H_2O_2 in preliminary experiments, rather than as a quantitative method for selectivity determination.

Table 1 provides an informative summary of the H_2O_2 detection methods discussed above. For electrochemically generated H_2O_2, the authors strongly recommend the use of RRDE if possible, as it provides a nearly instantaneous measurement of catalyst selectivity toward H_2O_2 and reduces the experimental variables present in the accumulation-based methods. Among accumulation methods, spectrophotometry

Please cite this article in press as: Shi et al., Electrochemical Synthesis of H_2O_2 by Two-Electron Water Oxidation Reaction, Chem (2020), https://doi.org/10.1016/j.chempr.2020.09.013

Table 1. Summary of H_2O_2 Measurement Techniques Utilized in Electrochemical Studies

	Method	Assays	Lower Detection Limit (ppm)	Pros	Cons
In situ	RRDE	N/A	setup dependent	not impacted by H_2O_2 stability	requires equipment, calibration
Accumulation-based	Titration	permanganate, ceric sulfate, Ti-based	1,000–10,000	no calibration, no equipment required	endpoint ambiguity, high lower detection limit
	spectro-photometry	Fe-based, Cu-based, cobalt-carbonate	0.3–4	low minimum detection limit, highly quantitative	potential for interference, temporal stability unknown
	colorimetric strips	proprietary	0.5–1,000 s	facile	time-sensitive, interference prone, poor accuracy

Source: Brandhuber and Korshin 2009.[76] Reprinted with permission. © WaterReuse Foundation

is preferable due to its low minimum detection limit, though the calibration should be carefully prepared and species that may interfere with determination should be screened before measurement. For a detailed comparison of interference effects, pH impact, electrolyte compatibility, and accuracy of selected accumulation-based methods, readers are directed to the reference.[80]

Reporting Catalyst Performance for 2e-WOR

Using standardized experimental protocols and carefully quantifying H_2O_2, meaningful data can be obtained to compare catalyst performance between laboratories. Still, standardized reporting metrics need to be used to facilitate comparison. The non-selective and thermodynamically unfavorable nature of 2e-WOR makes the definition of the overpotential difficult, as the onset of the current may be attributed to 4e-WOR. Accordingly, a partial current density toward H_2O_2 ($J_{H_2O_2}$) should be reported as a function of voltage.[27] $J_{H_2O_2}$ can be calculated by multiplying the voltage-dependent FE_{2e-WOR} by the overall current density. Furthermore, as many water-oxidation studies use electrodes with complex geometries and large surface area, $J_{H_2O_2}$ should be reported both normalized by the electrochemically active surface area and the geometric area, as described by others.[81] Though $J = 10\ mA/cm^2_{geometric}$ has become a standard current density at which to evaluate the overpotential in the 4e-WOR literature, based on the FE_{2e-WOR} and characteristics reported so far in the 2e-WOR literature, we suggest defining the onset potential for 2e-WOR (V_{2e-WOR}) catalysts as the voltage at which $J_{H_2O_2} = 1\ mA/cm^2_{geometric}$, such that the overpotential for 2e-WOR ($\eta_{H_2O_2}$) is:

$$\eta_{H_2O_2} = V_{2e-WOR} - 1.76 \qquad \text{(Equation E4)}$$

where all quantities are in volts versus the reversible hydrogen electrode. As previously mentioned, FE_{2e-WOR}should be measured and reported as a function of applied bias for a wide range of potentials. Furthermore, because the current densities exhibited by reported electrocatalysts are often low, previous research has reported the molar H_2O_2 production rate, a critically important metric for applications. Note that $J_{H_2O_2}$ can be converted to the molar H_2O_2 production rate($\dot{M}_{H_2O_2}$, expressed in mmol/cm^2-sec) by $\dot{M}_{H_2O_2} = \frac{J_{H_2O_2}}{nF}$, where n is the stoichiometric electron transfer number (2), F is Faraday's constant, and $J_{H_2O_2}$ is expressed in mA/cm^2. Finally, comparing the stability of 2e-WOR catalysts has proven exceptionally difficult, as applied bias and selectivity vary greatly among reports. For applications, H_2O_2 production is the primary goal of catalyst development. Accordingly, stability should be measured at a potential at which appreciable H_2O_2 is produced, rather than at the same potential for each electrocatalyst. We suggest that CA stability tests be performed at V_{2e-WOR} for the material being studied. To prevent further faradic efficiency testing after stability assessment, the catalytic lifetime (τ_{cat}) can then be defined as the elapsed time at which the *overall* current density

Please cite this article in press as: Shi et al., Electrochemical Synthesis of H_2O_2 by Two-Electron Water Oxidation Reaction, Chem (2020), https://doi.org/10.1016/j.chempr.2020.09.013

decays to less than 80% of its initial value. We believe that reporting these two metrics ($\eta_{H_2O_2}$ and τ_{cat}) in future 2e-WOR studies will provide unified grounds on which to holistically compare catalyst performance and thereby encourage progress in the field.

Summarily, both accurate quantification of H_2O_2 and consistent reporting of catalyst performance have been lacking in many 2e-WOR reports. We believe it is crucially important for detailed experimental protocols to be developed and explicitly detailed in new studies and for established and standardized metrics to be reported diligently. This will lead to the development of superior materials and more consistent and reliable fundamental studies.

EXPERIMENTAL RESULTS OF 2E-WOR CATALYSTS WITH BENCHMARKING METRICS

Description of Electrocatalysts Tested for 2e-WOR

Since 2e-WOR requires high anodic bias capable of oxidizing materials, most of the investigated electrocatalysts are metal oxides. These include tungsten oxide (WO_3),[28] tin oxide (SnO_2),[28,31] titanium oxide (TiO_2),[20,28,29] undoped and Gd-doped bismuth vanadate ($BiVO_4$),[23,33] calcium stannate ($CaSnO_3$),[28,30,31] manganese oxide (MnO_x),[32] lanthanum oxide (La_2O_3),[68] zirconium dioxide (ZrO_2),[68] cobalt oxide (Co_3O_4),[26] and aluminum oxide (Al_2O_3).[23] Only very few materials other than metal oxides have been reported as 2e-WOR catalysts. One notable work was a 2004 study, which employed a carbon-based material as an anode, along with a Pt mesh as the charge collector.[21] This report was among the first proposed systems for producing H_2O_2 through 2e-WOR, while a more recent work on carbon-based materials for 2e-WOR has also been reported.[34]

Activity and Selectivity of Various Catalysts toward 2e-WOR

MnO_x was the first reported metal oxide electrocatalyst for 2e-WOR in 2012,[32] wherein Izgorodin et al. showed that MnO_x exhibits a low overpotential for WOR (150 mV at 1 mA cm^{-2}). Though H_2O_2 evolution was demonstrated in this work, it did not report the specific electrochemical onset and faradic efficiency values. In 2016, Fuku et al. tested ten metal oxides and found $BiVO_4$ to be the best among them in terms of the H_2O_2 production rate under a fixed applied charge (Figure 8).[30] This result is consistent with our recent study, in which we examined four metal-oxide species (WO_3, $BiVO_4$, SnO_2, TiO_2).[28] We found that WO_3 has the lowest onset potential to produce H_2O_2, but $BiVO_4$ has both the highest peak faradic efficiency (70%) and the peak production rate for H_2O_2. TiO_2 has the lowest activity and selectivity for 2e-WOR. Based on DFT screening efforts, we recently examined $CaSnO_3$[31] and ZnO[27] for 2e-WOR. Both oxides surpass the electrocatalytic performance of $BiVO_4$ (Figures 8A–8C). Importantly, the experimentally determined onset potential (Figure 8A) of these metal oxides track well with the onset potential trend predicted by DFT in Figure 4D.

Beyond studies on pristine metal oxides, several other materials have been pursued to further enhance the performance of 2e-WOR systems. One recent study used Pt/TiO_2 (anatase), as a photoelectrocatalyst to anodically produce H_2O_2,[18] resulting in an enhanced mass-based production rate compared with a commercial Pt/TiO_2 system. In another study, Co_3O_4 was used as a co-catalyst with TiO_2.[26] The TiO_2 coated with Co_3O_4 exhibited higher faradic efficiency (~27%) than TiO_2 alone (~5%). We also showed that doping $BiVO_4$ with gadolinium (Gd) further enhances both the activity and selectivity for 2e-WOR because the oxyphilic Gd shifts the OH adsorption energy toward the more favorable values[33] (Figure 8). Recently, Zhang et al.

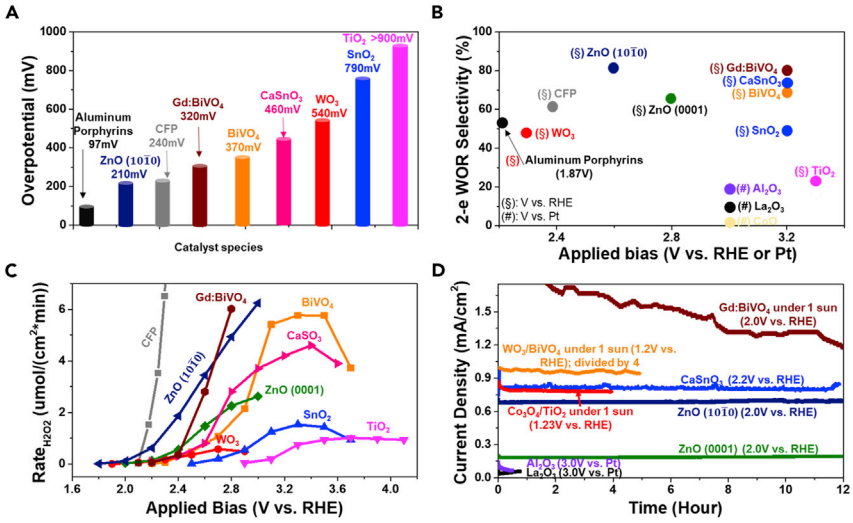

Figure 8. Summary of the Performance Metrics for the Reported Electrocatalysts for 2e-WOR

The electrolyte used is 2M $KHCO_3$.

(A) The overpotential for 2e-WOR, which is defined as the potential for H_2O_2 evolution onset (versus RHE) ($J_{H_2O_2} = 1\ mA/cm^2_{geometric}$) minus 1.76 V. Here, "CFP" stands for "carbon fiber paper" electrode from Xia et al.[34]

(B) The selectivity for H_2O_2 evolution as a function of applied bias.

(C) The H_2O_2 generation rate as a function of applied bias (versus RHE).

(D) The stability tests for different catalysts. Reprinted with permission from Fuku et al.[22] Copyright 2016 Royal Society of Chemistry. Reprinted with permission from Zhang et al.[26] Copyright 2018 Royal Society of Chemistry. Reprinted with permission from Shi et al.[28] Copyright 2017 Nature Publishing Group. Reprinted with permission from Mase et al.[30] Copyright 2016 Nature Publishing Group. Reprinted with permission from Park et al.[31] Copyright 2019 American Chemical Society. Reprinted with permission from Baek et al.[33] Copyright 2019 American Chemical Society. Reprinted with permission from Shi et al.[25] Copyright 2018 Royal Society of Chemistry. Reprinted with permission from Xia et al.[34] Copyright 2020 Nature Publishing Group. Reprinted with permission from Kuttassery et al.[36] Copyright 2017 John Wiley & Sons, Inc.

reported that the 2-electron and 4-electron competitive reactions can be transformed into the 1-electron and 2-electron competitive reactions by taking advantage of the Fermi-level pinning effect of the $BiVO_4$ photoanode, achieving 86% FE for H_2O_2 production.[82] This work opened up a possible strategy to suppress the thermodynamically favorable water-oxidative O_2 by kinetic controlling. Besides metal oxides or carbon materials, metal porphyrins have also been investigated for 2e-WOR.[35–37,83] In addition to new types of catalyst exploration, Wang et al. reported interfacial engineering using carbon catalysts as a model system with locally confined O_2 to greatly enhance the performance, and the approach was successfully extended to nickel.[34]

Some of the work discussed above was performed under illuminated conditions. We found that the faradic efficiency of $BiVO_4$ for 2e-WOR greatly improved under solar illumination, especially under lower bias.[28] For a fair comparison, Figures 8A–8C summarize all tests conducted without illumination to focus on the electrocatalytic properties. The figure indicates that metal porphyrins show good activity (overpotential as low as 97 mV) and selectivity ($[O_2]/[H_2O_2] = 0.31$).[36] Nevertheless, metal-porphyrin catalyst species are not stable even for short-term measurements,[84] and their stability needs to be significantly improved. While carbon-fiber paper (CFP) shows a higher reported H_2O_2 production rate (μmol min^{-1} cm^{-2}) than metal oxides,[34] it should be noted that the production rates are normalized based on

Please cite this article in press as: Shi et al., Electrochemical Synthesis of H_2O_2 by Two-Electron Water Oxidation Reaction, Chem (2020), https://doi.org/10.1016/j.chempr.2020.09.013

geometric areas. CFP's real surface area is much larger than its geometric surface area due to its porous nature, but most oxides investigated are thin films and their real surface area is close to their geometric surface area. A fair comparison for the production rate will be normalized by the real surface area. Metal oxides are the most studied oxides so far, in which ZnO and $BiVO_4$ are considered to be the best.

Most studies mentioned above employed a thin film of the catalyst on a conductive substrate to study the catalytic properties of metal oxides. A few studies have investigated the photoelectrochemical (PEC) properties of metal oxides, which require good optical, electrical, and catalytic properties for optimal performance. To further enhance light absorption, $WO_3/BiVO_4$ heterojunctions have been tested with enhanced nanostructures.[25] As a popular photoanode, $WO_3/BiVO_4$ is normally coupled with an oxygen-evolution catalyst for 4e-WOR.[85] However, since $BiVO_4$ has good catalytic properties toward 2e-WOR, $WO_3/BiVO_4$ core-shell structure with $BiVO_4$ as the shell is an excellent photoanode for H_2O_2 production.[22,25] The $WO_3/BiVO_4$ heterojunction, faradic efficiency, and production rate were further enhanced by depositing Al_2O_3, SiO_2, or ZrO_2 surface coatings,[23] which help reduce the degradation of generated H_2O_2.[23].

Stability of Electrocatalysts toward 2e-WOR

The stability of electrocatalysts is another important performance metric. WO_3 has a low onset potential for 2e-WOR but is known to be unstable in near neutral or alkaline conditions.[86] $BiVO_4$ is the most well-studied and high-performing catalyst for 2e-WOR, but its stability is also a major concern.[33] 2e-WOR requires high oxidizing potentials (>2V); whereas, $BiVO_4$ is highly unstable and vanadate anions dissolve into the electrolyte as previously discussed (Figure 5).[46,87] Doping $BiVO_4$ with other elements, such as Gd, was shown to improve its stability as oxyphilic Gd makes vanadate anions bind stronger to the surface.[33] The surface coating of other catalyst materials on $BiVO_4$, such as WO_3, to form the heterojunction also shows better stability.[22,25] The recently reported $CaSnO_3$ and ZnO have exhibited much better stability than $BiVO_4$ (Figure 8D) as well.[27,31] To date, faceted ZnO ($10\bar{1}0$) is the best electrocatalyst for 2e-WOR in terms of activity, selectivity, and stability.

As a brief conclusion, so far, metal oxides, metal porphyrins, and carbon materials have been used as catalysts for 2e-WOR, in which the carbon materials show the highest H_2O_2 production rate, and metal porphyrins show the lowest overpotential. Among those oxides, the faceted ZnO ($10\bar{1}0$) is the best so far. Nonetheless, the stability of those catalysts needs to be further evaluated and compared as stability is a prerequisite for practical applications.

OTHER IMPORTANT FACTORS AFFECTING 2E-WOR TO PRODUCE H_2O_2

In addition to the electrocatalyst material, other factors, such as electrolyte, temperature, H_2O_2 concentration, applied external bias, and impurities, can affect the catalytic performance for 2e-WOR. This section addresses the potential impact of electrolyte, H_2O_2 stability, and device configuration on 2e-WOR.

Effect of Electrolyte on 2e-WOR

The performance of 2e-WOR electrocatalysts is strongly affected by the electrolyte used. Studies by Fuku and Sayama et al. showed that bicarbonate ($KHCO_3$) electrolyte with near-neutral pH is the most effective electrolyte for H_2O_2 production (Figure 9).[22,88] The use of bicarbonate as the electrolyte leads to much

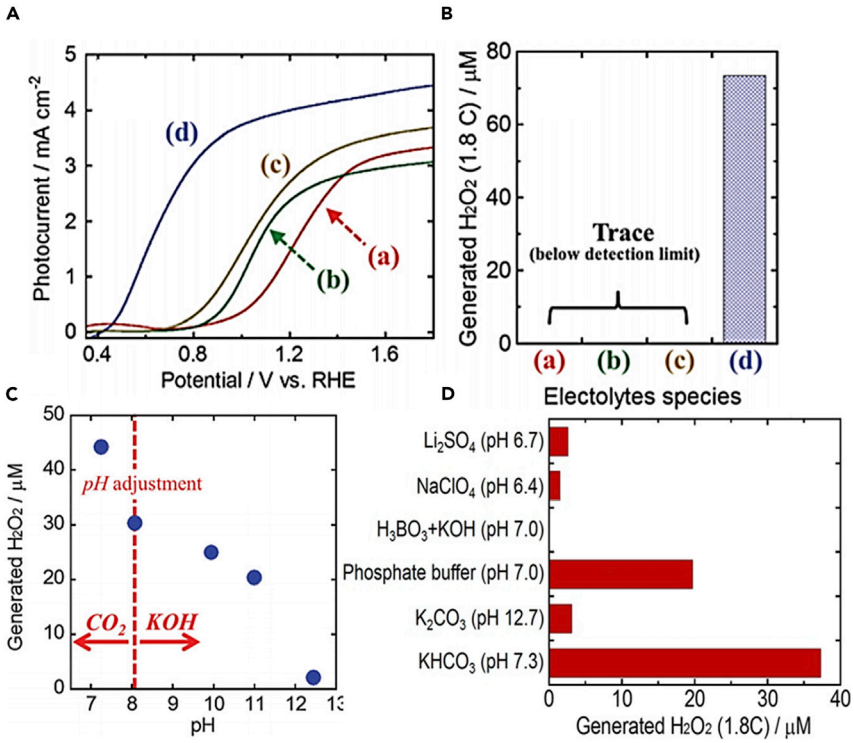

Figure 9. The Electrolyte Effect on 2e-WOR, Species, pH, and Concentration

(A) Shows the chemical composition effect to electrochemical current, in which the electrolytes (A)–(D) for four curves represent K_2SO_4, phosphate buffer, H_3BO_3, and $KHCO_3$, respectively, with the same concentration (0.5 M).

(B and C) (B) Chemical composition and concentration-effect to H_2O_2 selectivity, in which the electrolytes (A)–(D) are the same with what has been shown in (A); and (C) pH effect on H_2O_2 evolution, and the electrolyte used here is 0.5 M $KHCO_3$. (A)–(C) are tested on a $WO_3/BiVO_4$ electrode.

(D) The effects from all the three primary aspects to the final generated H_2O_2, which is tested on an FTO (fluorine-doped tin oxide) electrode.

(A–C) Reprinted with permission from Fuku et al.[22] Copyright 2016 Royal Society of Chemistry.

(D) Reprinted with permission from Fuku et al.[68] Copyright 2016 European Chemical Societies Publishing.

higher current density (Figure 9A) and the amount of H_2O_2 produced (Figure 9B) than other tested electrolytes, including K_2SO_4, phosphate buffer, and H_3BO_3. Most metal oxides reported have, therefore, used bicarbonate (HCO_3^-, such as $KHCO_3$ or $NaHCO_3$) as the electrolyte, likely due to its good performance.[22,23,25,26,28,30,31,33] Ando et al. and Izgorodin et al. reported that carbon-based catalysts perform best in NaOH, while MnO_x was used to evolve H_2O_2 with butyl ammonium bisulfate as the electrolyte.[21,32] All these studies showed that the choice of electrolyte affects the reported activity and selectivity of the electrocatalyst for 2e-WOR. This is different from studies on OER electrocatalysts, where the activity has mainly been attributed to the catalyst material, with the electrolyte playing the role of an ionic conductor only.

It is unclear how the electrolyte affects the electrocatalyst, which is one of the open questions for 2e-WOR. Some reports have hypothesized that bicarbonate works as a "redox catalyst."[89] Principally, bicarbonate anions (HCO_3^-) are oxidized to HCO_4^- (Equation 5A), and HCO_4^- subsequently oxidizes water to produce H_2O_2 while

Please cite this article in press as: Shi et al., Electrochemical Synthesis of H_2O_2 by Two-Electron Water Oxidation Reaction, Chem (2020), https://doi.org/10.1016/j.chempr.2020.09.013

being reduced back to HCO_3^- (Equation 5B).[22,90,91] Since the oxidation potential of $E^\circ(HCO_4^-/HCO_3^-) = 1.80$ V is nearly identical to that of $E^\circ(H_2O/H_2O_2) = 1.76$ V, the proposed bicarbonate redox catalyst is a plausible hypothesis, but further research is needed to be sure.

$$HCO_3^- + H_2O \leftrightarrow HCO_4^- + 2(H^+ + e^-) \quad \text{(Equation 5A)}$$

$$HCO_4^- + H_2O \leftrightarrow H_2O_2 + HCO_3^- \quad \text{(Equation 5B)}$$

Exploring this hypothesis or other possible mechanisms will require *operando* studies to determine the surface states and adsorbed species on the electrocatalysts. Current DFT methods typically do not consider the electrolyte, so new methodologies need to be developed to bridge the gap between the simplified DFT calculation setup and the complex experimental environment.

The pH and concentration of the electrolyte are known to affect the performance of 2e-WOR electrocatalysts through their impact on material stability, as discussed from a theoretical perspective in Predicting the Stability of Electrocatalysts under 2e-WOR Conditions, species concentration, and electrolyte conductivity (Figures 9C and 9D). Moreover, the electrolyte pH value also affects the stability of H_2O_2 as H_2O_2 is not stable under high pH, especially for alkaline solutions with pH > 12.0.[62] Previous studies on the effect of pH and concentration of bicarbonate on the generation rate of H_2O_2 show that near-neutral pH with higher bicarbonate concentrations (saturated solution, around 2M) is beneficial for H_2O_2 evolution from water oxidation.[30,91] Most metal oxides are stable in a near-neutral to slightly alkaline pH,[30] and some metal oxides, such as WO_3 as mentioned earlier, are only stable in weakly acidic solutions.[28] In this respect, since bicarbonate is a buffer to the near-neutral to slightly alkaline pH, it could be beneficial for the stability of most metal-oxide catalysts and for H_2O_2 production.[22] Nevertheless, bicarbonate is not a good electrolyte species for H_2O_2 storage,[24] as H_2O_2 can be consumed by oxidizing bicarbonate to HCO_4^- (the reverse reaction of Equation 5B).[24] H_2O_2 is stable in moderate acidic conditions, and little has been done on 2e-WOR for the acidic conditions due to the dominance of bicarbonate. New electrolytes, in addition to electrocatalysts, must be developed to produce H_2O_2 under acidic conditions.

Effect of Stability of H_2O_2 on Its Accumulation

In the last section, we discussed how H_2O_2 stability can be affected by electrolyte pH and the composition, especially in the case of HCO_3^-.[92] Moreover, H_2O_2 is intrinsically unstable. Several reaction pathways are responsible for the instability of H_2O_2: H_2O_2 disproportionation reaction to form H_2O and O_2,[62] electrochemical oxidation of H_2O_2 to O_2,[93] and chemical reduction of H_2O_2 to H_2O.[94] The disproportionation reaction rate was shown to increase with increasing temperature (Figure 10A), the impurity concentration (Figure 10B), and the H_2O_2 concentration (Figure 10C). First, the temperature dependence can be understood by the fact that the decomposition rate of H_2O_2 follows the Arrhenius equation and increases exponentially with temperature.[95] As expected, low temperature (i.e., using ice bath) was shown to be beneficial both for H_2O_2 production[22,30] and for preventing H_2O_2 decomposition (Figure 10A).[62,96] Second, impurities can catalyze the decomposition of H_2O_2. Figure 10B shows that metal ions promote H_2O_2 instability.[62] Any metals or metal ions in the electrochemical cell (i.e., Pt) may also accelerate H_2O_2 decomposition.[97] Impurities can be effectively alleviated by conventional alkaline peroxide-stabilizing agents, such as $MgSO_4$, Na_2SiO_3, and DTPA (diethylenetriamine pentaacetic acid).[98] Figure 10C shows that higher concentrations of H_2O_2 yield higher decomposition

Please cite this article in press as: Shi et al., Electrochemical Synthesis of H_2O_2 by Two-Electron Water Oxidation Reaction, Chem (2020), https://doi.org/10.1016/j.chempr.2020.09.013

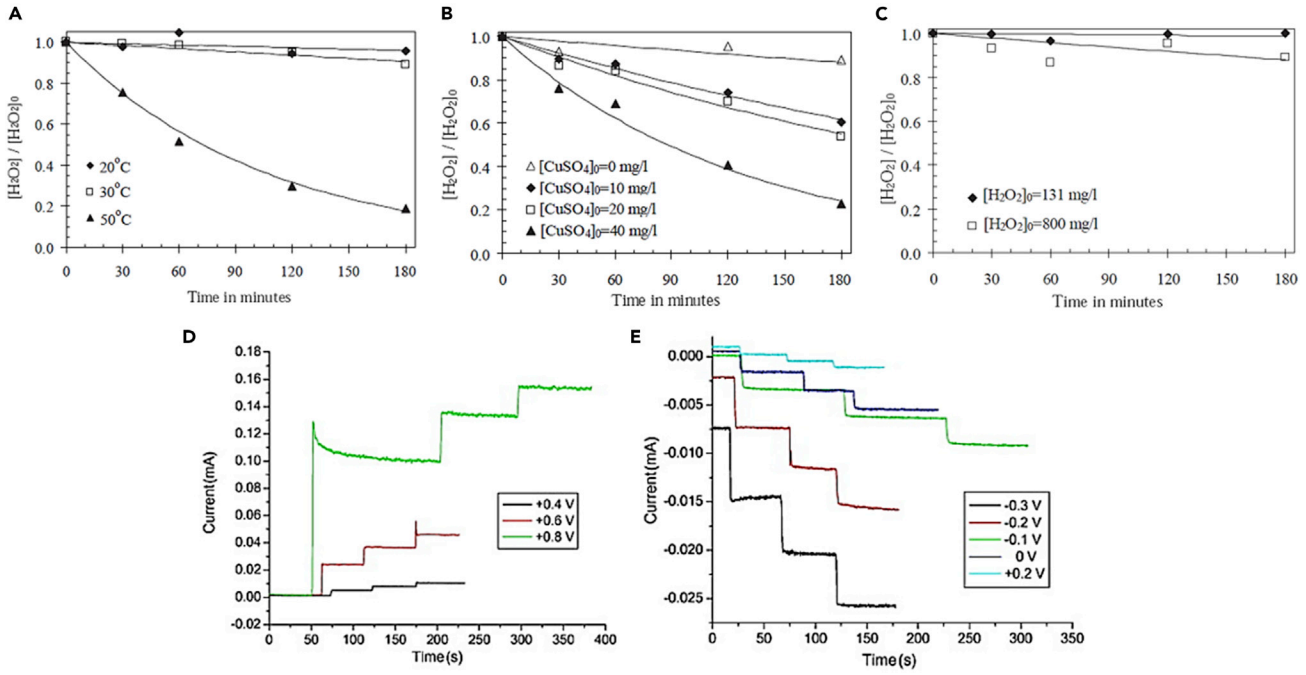

Figure 10. Summary of the Factors to the Stability of H_2O_2

The effects of temperature (A), impurity (B), and accumulated concentration of H_2O_2 (C), and the electrochemical oxidation (D) and reduction (E) under different external bias to H_2O_2.

(A–C) Measurements starting with a fixed concentration and test the decay ratio in terms of time, without external bias.

(D and E) Measurements of the amperometric response to three successive additions of 1 mM H_2O_2 to 0.01 M pH 7.4 phosphate buffer under different bias in an electrochemical cell, which aimed to study the effect of applied potentials on electrocatalytic oxidation and reduction of H_2O_2. The three additions of H_2O_2 correspond to three stepwise current responses observed for each curve. Here, the electrode material used is Co_3O_4 nanowalls electrode, and all applied potentials labeled in (D) and (E) are versus Ag/AgCl reference.

(A–C) Reprinted with permission from Yazici et al.[62] Copyright 2010 Proceedings of the XIIth. International mineral processing symposium.

(D and E) Reprinted with permission from Jia et al.[94] Copyright 2009 Elsevier.

rates.[62] A slower rate of H_2O_2 production was also observed when the accumulated H_2O_2 concentration gets higher in electrochemical cells.[24]

As pointed out above, in electrochemical systems H_2O_2 suffers not only from spontaneous disproportionation but could also undergo cathodic reduction to H_2O ($H_2O_2 + 2H^+ + 2e^- \rightarrow 2H_2O$; $E^o = 1.776$ V) (Figure 10D) or anodic oxidation to O_2 ($H_2O_2 \rightarrow O_2 + 2H^+ + 2e^-$; $E^o = 0.682$V) (Figure 10E).[94,99] Both figures show a sudden jump in current density whenever 1mM H_2O_2 is added to the system, indicating electrochemical reactions involving H_2O_2. Moreover, the magnitude of the current density is higher for the most positive bias in Figure 10D and the most negative bias in Figure 10E, indicating faster kinetic with higher bias. For 2e-WOR, higher anodic bias leads to faster production of H_2O_2 thermodynamically, but it also leads to the consumption of H_2O_2 by anodic oxidation. As a result, the faradic efficiency measured using the accumulated H_2O_2 concentration normally first increases and then decreases with increasing the applied bias.[28,31,33]

Design of the Electrochemical Cell for H_2O_2 Production

Besides the above fundamental studies on 2e-WOR, some studies have investigated the overall electrochemical device design for H_2O_2 production. At the device level, as we are focusing on anodic water oxidation to produce H_2O_2, the corresponding half-reaction induced at the cathode is the first means of distinction between devices. There are two popular choices. One cathodic reaction option is the hydrogen

Please cite this article in press as: Shi et al., Electrochemical Synthesis of H_2O_2 by Two-Electron Water Oxidation Reaction, Chem (2020), https://doi.org/10.1016/j.chempr.2020.09.013

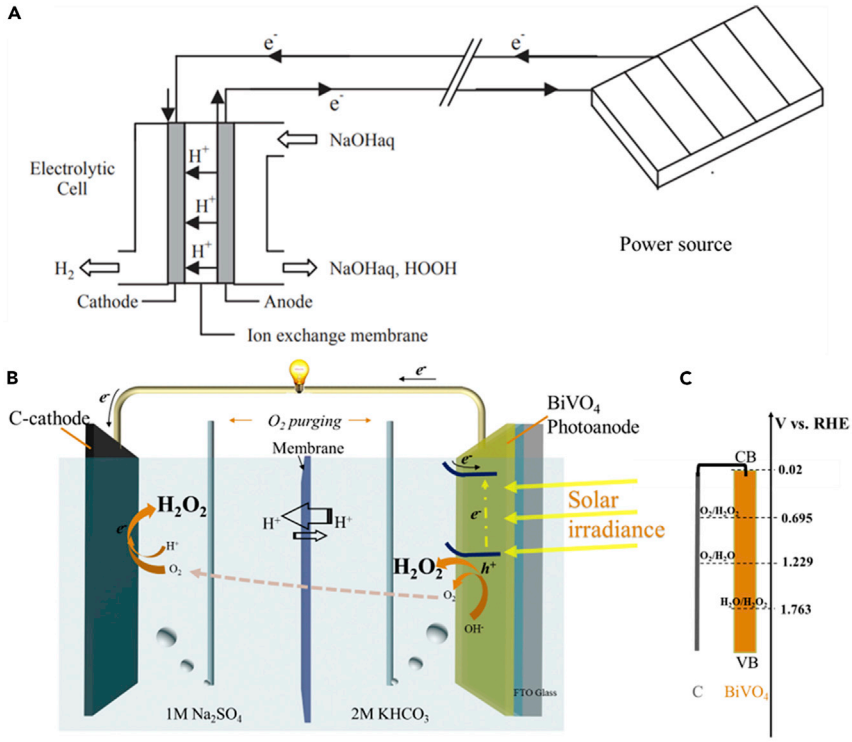

Figure 11. Schematic and Diagram for the Design of the Devices

(A) The device to produce H_2O_2 at the anode and H_2 at the cathode, using an electrical power source like a battery or a solar cell.

(B) The device to produce H_2O_2 from both sides, directly driven by solar energy.

(C) The band diagram of the system. The conduction band (CB) and valence band (VB) edge positions of $BiVO_4$ straddle the redox potentials of O_2/H_2O_2 and H_2O/H_2O_2, suggesting the possibility of unassisted H_2O_2 production.

(A) Reprinted with permission from Ando et al.[21] Copyright 2004 Elsevier.

(B and C) are reprinted with permission from Shi et al.[24] Copyright 2018 John Wiley & Sons, Inc.

evolution reaction (HER) to produce H_2 ($2H^+ + 2e^- = H_2$), which produces two valuable chemical species from a single electrochemical device (Figure 11A).[18,21] The other cathodic reaction option is the oxygen reduction reaction (ORR), where O_2 is purged into the system and reduced to H_2O through 4e-ORR and/or to H_2O_2 through 2e-ORR. 2e-ORR is preferred, as this will increase the amount of generated H_2O_2. Indeed, the two-sided H_2O_2 generation has been demonstrated (Figure 11B).[24,88] In addition to HER and ORR, other reduction reactions can be adopted at the cathode, which may endow these nascent devices with more potential uses and better performance.

In addition to the choice of cathode reactions, the electrochemical device can also be operated with or without solar illumination. Without solar illumination, the device is essentially an electrolyzer used to evolve H_2O_2. With solar illumination, the device is a PEC cell. Splitting water using PEC cells typically requires additional bias, and it is hard to find photoelectrodes that have band edges at sufficient potentials to straddle the 2e or 4e-WOR and HER equilibrium potentials. However, for 2e-ORR and 2e or 4e-WOR (in which 2e-WOR is more useful here), it is easier to find a photoelectrode for which the band edges straddle the H_2O/H_2O_2 (1.76 V versus RHE) and O_2/H_2O redox potentials, such as the $BiVO_4$ photoanode (Figure 11C). Two studies have demonstrated unassisted two-sided H_2O_2 production in a PEC cell.[24,88] Finally, solar energy and bias can be simultaneously applied to achieve a higher H_2O_2 yield.[24]

Please cite this article in press as: Shi et al., Electrochemical Synthesis of H_2O_2 by Two-Electron Water Oxidation Reaction, Chem (2020), https://doi.org/10.1016/j.chempr.2020.09.013

1e-WOR as a Competing Reaction

4e-WOR (i.e., OER) has been extensively studied, and 2e-WOR is receiving increasing attention. It is natural to consider the 1e-WOR toward the hydroxyl radical (OH•) production. OH• is a powerful oxidizer and, hence, is excellent for abating an array of contaminants. As discussed in Figure 4, 1e-WOR is thermodynamically preferred when the catalyst surface has a low free-binding energy of OH* relative to the formation energy of aqueous OH•. Theoretically, to the best of our knowledge, no electrocatalysts have been demonstrated to exhibit proper energetics for direct OH• generation. Furthermore, due to the high thermodynamic potential necessary to generate OH• (E° = 2.38 V_{RHE}), it will be difficult to find catalysts that are stable under such extreme anodic bias. Experimentally, due to its extraordinary reactivity, quantifying OH• concentration requires advanced analytical methods, such as spin trapping and fluorescence detection.[100]

The most commonly reported method for OH• generation is through the irradiation of TiO_2 photocatalysts.[69,101] Until recently, it was debated whether these radicals stemmed from water oxidation directly (i.e., the one-electron pathway) or from the reduction of generated H_2O_2 and O_2.[102] Evidence against the latter mechanism provides some hope that direct pathways toward 1e-WOR may be possible in photocatalytic and/or PEC systems, but much work remains in studying and establishing possible mechanisms and screening candidate materials.

As a brief conclusion, many other important factors are affecting 2e-WOR other than the stability and activity of the catalyst. In the future, researchers in this field should take care of these factors to better solve some fundamental issues or develop some downstream research directions.

SUMMARY AND OUTLOOK

In summary, the 2e-WOR provides an interesting pathway for distributed onsite H_2O_2 production under ambient conditions without gas-phase reactants. We reviewed the research progress on 2e-WOR, including basic principles, catalyst development, H_2O_2 detection, and system design.

On the theoretical side, DFT calculations have established principles to predict the activity, selectivity, and stability of 2e-WOR electrocatalysts, especially for metal oxides. ΔG_{OH*} was found to be the descriptor for the activity and selectivity of WOR in general. The preferred range of ΔG_{OH*} for 2e-WOR is between 1.6 and 2.4 eV, with the optimal value of 1.76 eV. The Pourbaix diagram is a great thermodynamic tool to predict the electrochemical stability of catalysts. Though the current DFT calculations for 2e-WOR shows good agreement with experiments, there is still room for improvement. First, most DFT simulations have only considered limited number of facets of oxides, while, in practice, many different facets exist in a polycrystalline oxide nanoparticle. Future studies should consider modeling more complicated facets of oxides, as high-index facets could also significantly contribute to the catalytic activity.[103] Second, electrochemical synthesis of H_2O_2 via 2e-WOR involves extreme oxidation potentials; therefore, stability of the catalyst materials is a crucial metric. Moving forward, research efforts should focus on identifying stable catalyst materials. With the recent developments in Pymatgen and Materials Project, Pourbiax diagrams can be rapidly constructed and used to evaluate the electrochemical stability. Third, considering the massive materials-phase space, high-throughput DFT calculation,[104] potentially coupled with machine learning, would be a game-changing strategy to identify stable and selective catalysts for 2e-WOR.

Please cite this article in press as: Shi et al., Electrochemical Synthesis of H_2O_2 by Two-Electron Water Oxidation Reaction, Chem (2020), https://doi.org/10.1016/j.chempr.2020.09.013

On the experimental side, many metal oxides have been tested as electrocatalysts for 2e-WOR, and their catalytic activity and selectivity generally agree with the DFT-predicted trends. Among those oxides, the faceted ZnO ($10\bar{1}0$) is the best so far. Carbon materials and metal porphyrins also show good results regarding the overpotential and the H_2O_2 production rate. Further research should orient more toward the materials exhibiting prolonged stability under 2e-WOR conditions. Moreover, the catalytic performance of 2e-WOR electrocatalysts and the accumulation of H_2O_2 are affected by many factors, including electrolyte choice, pH, accumulated H_2O_2 concentration, temperature, impurities, and external bias. Many of these factors and their mechanistic impacts have not been studied in detail, inviting further research in these areas. The complexity also calls for standardized experimental protocols and performance-reporting benchmarks, which are critical to furthering 2e-WOR electrocatalyst development. Finally, electrocatalysts alone will not lead to successful onsite production of H_2O_2. We need to have a device-level design of fuel cells, perhaps PEC cells as well, to optimize the accumulation of H_2O_2. Though 2e-WOR has enjoyed heightened attention from both theoretical and experimental research groups, and early results have shown the promise of metal oxides as catalyst materials, many fundamental questions require more exploration. Above all, the unification of methods in the field will be important in answering these questions rigorously and in pushing 2e-WOR toward device-level implementation.

So far, most studies on 2e-WOR have been focused on fundamental discoveries of electrocatalysts. There is a long path toward practical applications, which require stable and nontoxic catalysts. Longer or accelerated tests need to be carried out to understand the stability of catalysts and accumulated H_2O_2. Also, methods need to be developed to stabilize and separate the accumulated H_2O_2 from the electrolyte to extend its use for different purposes. For example, the produced H_2O_2 may need to be coupled with Fenton reaction or UV illumination for effective water disinfection. Finally, the cost for distributed production/application of H_2O_2 needs to be competitive with centralized production and distributed application. One previous research showed that the cost to produce 1kg H_2 is way more superior when producing H_2O_2 instead of O_2 at the anode,[105] considering the averaged market value of \$0.85 kg^{-1} for H_2O_2. Nonetheless, techno-economic analysis and life cycle analysis need to be conducted to understand the practicality of onsite H_2O_2 production.

AUTHOR CONTRIBUTIONS

S.S. and X.Z. conceived the idea and devised the review structure. X.S., T.G., and X.Z. investigated the literature and prepared the experimental sections, from Experimental Methods for Characterizing 2e-WOR Catalysts to Important Factors Affecting 2e-WOR to Produce H_2O_2; S.B. and S.S. investigated the literature and prepared the theoretical section, Theoretical Aspects for the Rational Design of 2e-WOR Catalysts. All authors contributed in writing the Summary, Introduction, and Summary and Outlook.

ACKNOWLEDGMENTS

S.S. gratefully acknowledges the support from the University of Calgary Seed Grant and the University of Calgary's Canada First Research Excellence Fund Program, the Global Research Initiative in Sustainable Low Carbon Unconventional Resources. X.Z. thanks the Stanford Woods Institute for the Environment, the Stanford Natural Gas Initiative, and the Stanford Tomkat Center for their generous support. T.M.G. would like to thank the National Science Foundation for their support

through the Graduate Research Fellowship Program and Stanford University for their support through the Stanford Graduate Fellowship in Science and Engineering. S.B. acknowledges the support from the National Research Foundation of Korea (NRF) funded by the Ministry of Science and ICT (2015M3D3A1A01064929).

REFERENCES

1. Cai, J.Y., Evans, D.J., and Smith, S.M. (2001). Bleaching of natural fibers with TAED and NOBS activated peroxide systems. AATCC Rev *1*, 31–34.

2. Sheldon, R. (2012). Metal-Catalyzed Oxidations of Organic Compounds: Mechanistic Principles and Synthetic Methodology Including Biochemical Processes (Elsevier).

3. Wilmotte, R., Lebeau, B., Irurzun, J.-P., and Marechal, F. (2003). Disinfecting composition based on H2O2, acids and metal ions. US Patent USOO6660289B1, filed April 25, 2000, and granted December 9, 2003.

4. Campos-Martin, J.M., Blanco-Brieva, G., and Fierro, J.L. (2006). Hydrogen peroxide synthesis: an outlook beyond the anthraquinone process. Angew. Chem. Int. Ed. Engl. *45*, 6962–6984.

5. Samanta, C., and Choudhary, V.R. (2007). Direct formation of H2O2 from H2 and O2 and decomposition/hydrogenation of H2O2 in aqueous acidic reaction medium over halide-containing Pd/SiO2 catalytic system. Cat. Commun. *8*, 2222–2228.

6. Solsona, B.E., Edwards, J.K., Landon, P., Carley, A.F., Herzing, A., Kiely, C.J., and Hutchings, G.J. (2006). Direct synthesis of hydrogen peroxide from H2 and O2 using Al 2 O3 supported Au—Pd catalysts. Chem. Mater. *18*, 2689–2695.

7. Xia, C., Xia, Y., Zhu, P., Fan, L., and Wang, H. (2019). Direct electrosynthesis of pure aqueous H2O2 solutions up to 20% by weight using a solid electrolyte. Science *366*, 226–231.

8. Sánchez-Sánchez, C.M., and Bard, A.J. (2009). Hydrogen peroxide production in the oxygen reduction reaction at different electrocatalysts as quantified by scanning electrochemical microscopy. Anal. Chem. *81*, 8094–8100.

9. Nørskov, J.K., Rossmeisl, J., Logadottir, A., Lindqvist, L., Kitchin, J.R., Bligaard, T., and Jónsson, H. (2004). Origin of the overpotential for oxygen reduction at a fuel-cell cathode. J. Phys. Chem. B *108*, 17886–17892.

10. Qu, L., Liu, Y., Baek, J.B., and Dai, L. (2010). Nitrogen-doped graphene as efficient metal-free electrocatalyst for oxygen reduction in fuel cells. ACS Nano *4*, 1321–1326.

11. Siahrostami, S., Verdaguer-Casadevall, A., Karamad, M., Deiana, D., Malacrida, P., Wickman, B., Escudero-Escribano, M., Paoli, E.A., Frydendal, R., Hansen, T.W., et al. (2013). Enabling direct H2O2 production through rational electrocatalyst design. Nat. Mater. *12*, 1137–1143.

12. Chen, S., Chen, Z., Siahrostami, S., Kim, T.R., Nordlund, D., Sokaras, D., Nowak, S., To, J.W.F., Higgins, D., Sinclair, R., et al. (2018). Defective carbon-based materials for the electrochemical synthesis of hydrogen peroxide. ACS Sustainable Chem. Eng. *6*, 311–317.

13. Jiang, K., Back, S., Akey, A.J., Xia, C., Hu, Y., Liang, W., Schaak, D., Stavitski, E., Nørskov, J.K., Siahrostami, S., and Wang, H. (2019). Highly selective oxygen reduction to hydrogen peroxide on transition metal single atom coordination. Nat. Commun. *10*, 3997.

14. Qiang, Z., Chang, J.H., and Huang, C.P. (2002). Electrochemical generation of hydrogen peroxide from dissolved oxygen in acidic solutions. Water Res *36*, 85–94.

15. Lu, Z., Chen, G., Siahrostami, S., Chen, Z., Liu, K., Xie, J., Liao, L., Wu, T., Lin, D., Liu, Y., et al. (2018). High-efficiency oxygen reduction to hydrogen peroxide catalysed by oxidized carbon materials. Nat. Cat. *1*, 156–162.

16. Jiang, Y., Ni, P., Chen, C., Lu, Y., Yang, P., Kong, B., Fisher, A., and Wang, X. (2018). Selective Electrochemical H2 O2 production through two-electron oxygen electrochemistry. Adv. Energy Mater. *8*, 1801909.

17. Fukuzumi, S., Lee, Y.M., and Nam, W. (2018). Solar-driven production of hydrogen peroxide from water and dioxygen. Chemistry *24*, 5016–5031.

18. Wang, L., Cao, S., Guo, K., Wu, Z., Ma, Z., and Piao, L. (2019). Simultaneous hydrogen and peroxide production by photocatalytic water splitting. Chin. J. Cat *40*, 470–475.

19. Shiraishi, F., Nakasako, T., and Hua, Z. (2003). Formation of hydrogen peroxide in photocatalytic reactions. J. Phys. Chem. A *107*, 11072–11081.

20. Shiraishi, Y., Kanazawa, S., Tsukamoto, D., Shiro, A., Sugano, Y., and Hirai, T. (2013). Selective hydrogen peroxide formation by titanium dioxide photocatalysis with benzylic alcohols and molecular oxygen in water. ACS Catal *3*, 2222–2227.

21. Ando, Y., and Tanaka, T. (2004). Proposal for a new system for simultaneous production of hydrogen and hydrogen peroxide by water electrolysis. Int. J. Hydr. Energy *29*, 1349–1354.

22. Fuku, K., and Sayama, K. (2016). Efficient oxidative hydrogen peroxide production and accumulation in photoelectrochemical water splitting using a tungsten trioxide/bismuth vanadate photoanode. Chem. Commun. (Camb.) *52*, 5406–5409.

23. Fuku, K., Miyase, Y., Miseki, Y., Gunji, T., and Sayama, K. (2017). WO3/BiVO4 photoanode coated with mesoporous Al2O3 layer for oxidative production of hydrogen peroxide from water with high selectivity. RSC Adv *7*, 47619–47623.

24. Shi, X., Zhang, Y., Siahrostami, S., and Zheng, X. (2018). Light-driven BiVO4–C fuel cell with simultaneous production of H2O2. Adv. Energy Mater. *8*, 1801158.

25. Shi, X., Cai, L., Choi, I.Y., Ma, M., Zhang, K., Zhao, J., Kim, J.K., Kim, J.K., Zheng, X., and Park, J.H. (2018). Epitaxial growth of WO3 nanoneedles achieved using a facile flame surface treatment process engineering of hole transport and water oxidation reactivity. J. Mater. Chem. A *6*, 19542–19546.

26. Zhang, J., Chang, X., Luo, Z., Wang, T., and Gong, J. (2018). A highly efficient photoelectrochemical H2O2 production reaction with Co3O4 as a co-catalyst. Chem. Commun. (Camb.) *54*, 7026–7029.

27. Kelly, S.R., Shi, X., Back, S., Vallez, L., Park, S.Y., Siahrostami, S., Zheng, X., and Nørskov, J.K. (2019). ZnO as an active and selective catalyst for electrochemical water oxidation to hydrogen peroxide. ACS Catal *9*, 4593–4599.

28. Shi, X., Siahrostami, S., Li, G.L., Zhang, Y., Chakthranont, P., Studt, F., Jaramillo, T.F., Zheng, X., and Nørskov, J.K. (2017). Understanding activity trends in electrochemical water oxidation to form hydrogen peroxide. Nat. Commun. *8*, 701.

29. Siahrostami, S., Li, G.L., Viswanathan, V., and Nørskov, J.K. (2017). One-or two-electron water oxidation, hydroxyl radical, or H2O2 evolution. J. Phys. Chem. Lett. *8*, 1157–1160.

30. Mase, K., Yoneda, M., Yamada, Y., and Fukuzumi, S. (2016). Seawater usable for production and consumption of hydrogen peroxide as a solar fuel. Nat. Commun. *7*, 11470.

31. Park, S.Y., Abroshan, H., Shi, X., Jung, H.S., Siahrostami, S., and Zheng, X. (2019). CaSnO3: an electrocatalyst for 2-electron water oxidation reaction to form H2O2. ACS Energy Lett *4*, 352–357.

32. Izgorodin, A., Izgorodina, E., and MacFarlane, D.R. (2012). Low overpotential water oxidation to hydrogen peroxide on a MnO x catalyst. Energy Environ. Sci. *5*, 9496–9501.

33. Baek, J.H., Gill, T.M., Abroshan, H., Park, S., Shi, X., Nørskov, J.K., Jung, H.S., Siahrostami, S., and Zheng, X. (2019). Selective and efficient Gd-doped BiVO4 photoanode for two-electron water oxidation to H2O2. ACS Energy Lett *4*, 720–728.

34. Xia, C., Back, S., Ringe, S., Jiang, K., Chen, F.H., Sun, X.M., Siahrostami, S., Chan, K.R., and Wang, H.T. (2020). Confined local oxygen gas promotes electrochemical water

oxidation to hydrogen peroxide. Nat. Cat. *3*, 125–134.

35. Liu, Y., Han, Y., Zhang, Z., Zhang, W., Lai, W., Wang, Y., and Cao, R. (2019). Low overpotential water oxidation at neutral pH catalyzed by a copper (II) porphyrin. Chem. Sci. *10*, 2613–2622.

36. Kuttassery, F., Mathew, S., Sagawa, S., Remello, S.N., Thomas, A., Yamamoto, D., Onuki, S., Nabetani, Y., Tachibana, H., and Inoue, H. (2017). One electron-initiated two-electron oxidation of water by aluminum porphyrins with earth's most abundant metal. ChemSusChem *10*, 1909–1915.

37. Kuttassery, F., Mathew, S., Tachibana, H., and Inoue, H. (2020). How one-photon can induce water splitting into hydrogen peroxide and hydrogen by aluminum porphyrins. Rationale of the thermodynamics. Sustain. Energy Fuels *4*, 1945–1953.

38. Bard, A. (2017). Standard Potentials in Aqueous Solution (Routledge).

39. Pellegrini, F., Montangero, S., Santoro, G.E., and Fazio, R. (2008). Adiabatic quenches through an extended quantum critical region. Phys. Rev. B *77*, 140404.

40. Krishnamurthy, D., Sumaria, V., and Viswanathan, V. (2019). Quantifying robustness of DFT predicted pathways and activity determining elementary steps for electrochemical reactions. J. Chem. Phys. *150*, 041717.

41. Abild-Pedersen, F., Greeley, J., Studt, F., Rossmeisl, J., Munter, T.R., Moses, P.G., Skúlason, E., Bligaard, T., and Nørskov, J.K. (2007). Scaling properties of adsorption energies for hydrogen-containing molecules on transition-metal surfaces. Phys. Rev. Lett. *99*, 016105.

42. Man, I.C., Su, H.Y., Calle-Vallejo, F., Hansen, H.A., Martínez, J.I., Inoglu, N.G., Kitchin, J., Jaramillo, T.F., Nørskov, J.K., and Rossmeisl, J. (2011). Universality in oxygen evolution electrocatalysis on oxide surfaces. ChemCatChem *3*, 1159–1165.

43. Kulkarni, A., Siahrostami, S., Patel, A., and Nørskov, J.K. (2018). Understanding catalytic activity trends in the oxygen reduction reaction. Chem. Rev. *118*, 2302–2312.

44. Ong, S.P., Richards, W.D., Jain, A., Hautier, G., Kocher, M., Cholia, S., Gunter, D., Chevrier, V.L., Persson, K.A., and Ceder, G. (2013). Python materials genomics (pymatgen): a robust, open-source python library for materials analysis. Comp. Mater. Sci. *68*, 314–319.

45. Jain, A., Ong, S.P., Hautier, G., Chen, W., Richards, W.D., Dacek, S., Cholia, S., Gunter, D., Skinner, D., Ceder, G., and Persson, K.A. (2013). Commentary: the materials project: a materials genome approach to accelerating materials innovation. Apl. Mater. *1*, 011002.

46. Toma, F.M., Cooper, J.K., Kunzelmann, V., McDowell, M.T., Yu, J., Larson, D.M., Borys, N.J., Abelyan, C., Beeman, J.W., Yu, K.M., et al. (2016). Mechanistic insights into chemical and photochemical transformations of bismuth vanadate photoanodes. Nat. Commun. *7*, 12012.

47. Franchini, C., Podloucky, R., Paier, J., Marsman, M., and Kresse, G. (2007). Ground-state properties of multivalent manganese oxides: density functional and hybrid density functional calculations. Phys. Rev. B *75*, 195128.

48. Dudarev, S.L., Botton, G.A., Savrasov, S.Y., Humphreys, C.J., and Sutton, A.P. (1998). Electron-energy-loss spectra and the structural stability of nickel oxide: an LSDA+ U study. Phys. Rev. B *57*, 1505–1509.

49. Cococcioni, M., and De Gironcoli, S. (2005). Linear response approach to the calculation of the effective interaction parameters in the LDA+ U method. Phys. Rev. B *71*, 035105.

50. Xu, Z., Rossmeisl, J., and Kitchin, J.R. (2015). A linear response DFT+ U study of trends in the oxygen evolution activity of transition metal rutile dioxides. J. Phys. Chem. C *119*, 4827–4833.

51. Wellendorff, J., Silbaugh, T.L., Garcia-Pintos, D., Nørskov, J.K., Bligaard, T., Studt, F., and Campbell, C.T. (2015). A benchmark database for adsorption bond energies to transition metal surfaces and comparison to selected DFT functionals. Surf. Sci. *640*, 36–44.

52. Chuasiripattana, K., Warschkow, O., Delley, B., and Stampfl, C. (2010). Reaction intermediates of methanol synthesis and the water–gas-shift reaction on the ZnO (0001) surface. Surf. Sci. *604*, 1742–1751.

53. Medford, A.J., Sehested, J., Rossmeisl, J., Chorkendorff, I., Studt, F., Nørskov, J.K., and Moses, P.G. (2014). Thermochemistry and micro-kinetic analysis of methanol synthesis on ZnO (0 0 0 1). J. Cat *309*, 397–407.

54. Siahrostami, S., Björketun, M.E., Strasser, P., Greeley, J., and Rossmeisl, J. (2013). Tandem cathode for proton exchange membrane fuel cells. Phys. Chem. Chem. Phys. *15*, 9326–9334.

55. Greeley, J., Stephens, I.E., Bondarenko, A.S., Johansson, T.P., Hansen, H.A., Jaramillo, T.F., Rossmeisl, J., Chorkendorff, I., and Nørskov, J.K. (2009). Alloys of platinum and early transition metals as oxygen reduction electrocatalysts. Nat. Chem. *1*, 552–556.

56. He, Z.D., Hanselman, S., Chen, Y.X., Koper, M.T.M., and Calle-Vallejo, F. (2017). Importance of solvation for the accurate prediction of oxygen reduction activities of Pt-based electrocatalysts. J. Phys. Chem. Lett. *8*, 2243–2246.

57. Casalongue, H.S., Kaya, S., Viswanathan, V., Miller, D.J., Friebel, D., Hansen, H.A., Nørskov, J.K., Nilsson, A., and Ogasawara, H. (2013). Direct observation of the oxygenated species during oxygen reduction on a platinum fuel cell cathode. Nat. Commun. *4*, 1–6.

58. Siahrostami, S., and Vojvodic, A. (2015). Influence of adsorbed water on the oxygen evolution reaction on oxides. J. Phys. Chem. C *119*, 1032–1037.

59. McCrory, C.C.L., Jung, S.H., Peters, J.C., and Jaramillo, T.F. (2013). Benchmarking heterogeneous electrocatalysts for the oxygen evolution reaction. J. Am. Chem. Soc. *135*, 16977–16987.

60. Huynh, M., Shi, C.Y., Billinge, S.J.L., and Nocera, D.G. (2015). Nature of activated manganese oxide for oxygen evolution. J. Am. Chem. Soc. *137*, 14887–14904.

61. Sillanpaa, M., and Shestakova, M. (2017). Introduction. Electrochemical Water Treatment Methods: Fundamentals, Methods and Full Scale Applications. pp. 1–46.

62. Yazici, E., and Deveci, H. (2010). Factors affecting decomposition of hydrogen peroxide. In Proceedings of the XIIth International Mineral Processing Symposium, pp. 6–10.

63. Huckaba, C.E., and Keyes, F.G. (1948). The accuracy of estimation of hydrogen peroxide by potassium permanganate titration. J. Am. Chem. Soc. *70*, 1640–1644.

64. Mathieson, D.W. (1967). In Standard methods of chemical analysis. Instrumental analysis, 6th edition, *19*, F.J. Welcher, ed. (J. Pharm. Pharmacol.), p. 72.

65. Marquette, C.A., and Blum, L.J. (2006). Applications of the luminol chemiluminescent reaction in analytical chemistry. Anal. Bioanal. Chem. *385*, 546–554.

66. Keston, A.S., and Brandt, R. (1965). The fluorometric analysis of ultramicro quantities of hydrogen peroxide. Anal. Biochem. *11*, 1–5.

68. Fuku, K., Miyase, Y., Miseki, Y., Gunji, T., and Sayama, K. (2016). Enhanced oxidative hydrogen peroxide production on conducting glass anodes modified with metal oxides. ChemistrySelect *1*, 5721–5726.

69. Hirakawa, T., Yawata, K., and Nosaka, Y. (2007). Photocatalytic reactivity for O2− and OH radical formation in anatase and rutile TiO2 suspension as the effect of H2O2 addition. Appl. Cat. A *325*, 105–111.

70. Prater, K.B., and Bard, A.J. (1970). Rotating ring-disk Electrodes .3. J. Electrochem. Soc. *117*, 1517.

71. Antoine, O., and Durand, R. (2000). RRDE study of oxygen reduction on Pt nanoparticles inside nafion (R): H2O2 production in PEMFC cathode conditions. Journal of Applied Electrochemistry *30*, 839–844.

72. Zhou, R.F., Zheng, Y., Jaroniec, M., and Qiao, S.Z. (2016). Determination of the electron transfer number for the oxygen reduction reaction: from theory to experiment. ACS Catal *6*, 4720–4728.

73. Xia, C., Kim, J.Y., and Wang, H. (2020). Recommended practice to report selectivity in electrochemical synthesis of H2O2. Nat. Cat. *3*, 605–607.

74. Mase, K., Yoneda, M., Yamada, Y., and Fukuzumi, S. (2016). Efficient photocatalytic production of hydrogen peroxide from water and dioxygen with bismuth vanadate and a cobalt(II) chlorin complex. ACS Energy Lett *1*, 913–919.

75. Chen, Z.H., Chen, S.C., Siahrostami, S., Chakthranont, P., Hahn, C., Nordlund, D., Dimosthenis, S., Nørskov, J.K., Bao, Z.N., and Jaramillo, T.F. (2017). Development of a reactor with carbon catalysts for modular-

scale, low-cost electrochemical generation of H2O2. React. Chem. Eng. *2*, 239–245.

76. Brandhuber, P., and Korshin, G.V. (2009). Methods for the detection of residual concentations of hydrogen peroxide in advanced oxidation processes (WaterReuse Foundation). https://watereuse.org/watereuse-research/04-19-methods-for-detection-of-residual-concentrations-of-hydrogen-peroxide-in-advanced-oxidation-processes-2/.

77. Baga, A.N., Johnson, G.R.A., Nazhat, N.B., Saadalla-Nazhat, R.A., and Simple, A. (1988). A simple spectrophotometric determination of hydrogen peroxide at low concentrations in aqueous solution. Anal. Chim. Acta *204*, 349–353.

78. Belhateche, D., and Symons, J.M. (1991). Using cobalt-ultraviolet spectrophotometry to measure hydrogen peroxide concentration in organically laden groundwaters. J. Am. Water Works Assoc. *83*, 70–73.

79. Brandhuber, P., Clark, S., and Morley, K. (2009). A review of perchlorate occurrence in public drinking water systems. J. Am. Water Works Assoc. *101*, 63–73.

80. Gill, T.M., and Zheng, X. (2020). Comparing methods for quantifying electrochemically accumulated H2O2. Chem. Mater. *32*, 6285–6294.

81. Voiry, D., Chhowalla, M., Gogotsi, Y., Kotov, N.A., Li, Y., Penner, R.M., Schaak, R.E., and Weiss, P.S. (2018). Best practices for reporting electrocatalytic performance of nanomaterials. ACS Nano *12*, 9635–9638.

82. Zhang, K., Liu, J., Wang, L., Jin, B., Yang, X., Zhang, S., and Park, J.H. (2020). Near-complete suppression of oxygen evolution for photoelectrochemical H2O oxidative H2O2 synthesis. J. Am. Chem. Soc. *142*, 8641–8648.

83. Kuttassery, F., Sagawa, S., Mathew, S., Nabetani, Y., Iwase, A., Kudo, A., Tachibana, H., and Inoue, H. (2019). Water splitting on aluminum porphyrins to form hydrogen and hydrogen peroxide by one photon of visible light. ACS Appl. Energy Mater. *2*, 8045–8051.

84. Perry, S.C., Pangotra, D., Vieira, L., Csepei, L.-I., Sieber, V., Wang, L., Ponce de León, C.P., and Walsh, F.C. (2019). Electrochemical synthesis of hydrogen peroxide from water and oxygen. Nat. Rev. Chem. *3*, 442–458.

85. Rao, P.M., Cai, L., Liu, C., Cho, I.S., Lee, C.H., Weisse, J.M., Yang, P., and Zheng, X. (2014). Simultaneously efficient light absorption and charge separation in WO3/BiVO4 core/shell nanowire photoanode for photoelectrochemical water oxidation. Nano Lett *14*, 1099–1105.

86. Hill, J.C., and Choi, K.-S. (2012). Effect of electrolytes on the selectivity and stability of n-type WO3 photoelectrodes for use in solar water oxidation. J. Phys. Chem. C *116*, 7612–7620.

87. Tolod, K., Hernández, S., and Russo, N. (2017). Recent advances in the BiVO4 photocatalyst for sun-driven water oxidation: top-performing photoanodes and scale-up challenges. Catalysts *7*, 13.

88. Fuku, K., Miyase, Y., Miseki, Y., Funaki, T., Gunji, T., and Sayama, K. (2017). Photoelectrochemical hydrogen peroxide production from water on a WO3/BiVO4 photoanode and from O2 on an Au cathode without external bias. Chem. Asian J. *12*, 1111–1119.

89. Miseki, Y., and Sayama, K. (2019). Photocatalytic water splitting for solar hydrogen production using the carbonate effect and the Z-scheme reaction. Adv. Energy Mater. *9*, 1801294.

90. Richardson, D.E., Yao, H., Frank, K.M., and Bennett, D.A. (2000). Equilibria, kinetics, and mechanism in the bicarbonate activation of hydrogen peroxide: oxidation of sulfides by peroxymonocarbonate. J. Am. Chem. Soc. *122*, 1729–1739.

91. Shi, X., Choi, I.Y., Zhang, K., Kwon, J., Kim, D.Y., Lee, J.K., Oh, S.H., Kim, J.K., and Park, J.H. (2014). Efficient photoelectrochemical hydrogen production from bismuth vanadate-decorated tungsten trioxide helix nanostructures. Nat. Commun. *5*, 4775.

92. Simoyi, R.H., De Kepper, P., Epstein, I.R., and Kustin, K. (1986). Reaction between permanganate ion and hydrogen peroxide: kinetics and mechanism of the initial phase of the reaction. Inorg. Chem. *25*, 538–542.

93. Hall, S.B., Khudaish, E.A., and Hart, A.L. (1998). Electrochemical oxidation of hydrogen peroxide at platinum electrodes. Part 1. An adsorption-controlled mechanism. Electrochim. Acta *43*, 579–588.

94. Jia, W., Guo, M., Zheng, Z., Yu, T., Rodriguez, E.G., Wang, Y., and Lei, Y. (2009). Electrocatalytic oxidation and reduction of H2O2 on vertically aligned Co3O4 nanowalls electrode: toward H2O2 detection. J. Electroanal. Chem. *625*, 27–32.

95. Beers, R.F., and Sizer, I.W. (1952). A spectrophotometric method for measuring the breakdown of hydrogen peroxide by catalase. J. Biol. Chem. *195*, 133–140.

96. Zun, M., Dwornicka, D., Wojciechowska, K., Swiader, K., Kasperek, R., Rzadkowska, M., and Poleszak, E. (2014). Kinetics of the decomposition and the estimation of the stability of 10% aqueous and non-aqueous hydrogen peroxide solutions. Curr. Issues Pharm. Med. Sci. *27*, 213–216.

97. Laursen, A.B., Man, I.C., Trinhammer, O.L., Rossmeisl, J., and Dahl, S. (2011). The Sabatier principle illustrated by catalytic H2O2 decomposition on metal surfaces. J. Chem. Educ. *88*, 1711–1715.

98. Lee, H.B.H., Park, A.-H., and Oloman, W.C. (2000). Stability of hydrogen peroxide in sodium carbonate solutions. Tappi J *83*, 1–9.

99. Stewart, K.L., and Gewirth, A.A. (2007). Mechanism of electrochemical reduction of hydrogen peroxide on copper in acidic sulfate solutions. Langmuir *23*, 9911–9918.

100. Zhang, J., and Nosaka, Y. (2013). Quantitative detection of OH radicals for investigating the reaction mechanism of various visible-light TiO2 photocatalysts in aqueous suspension. J. Phys. Chem. C *117*, 1383–1391.

101. Goto, H., Hanada, Y., Ohno, T., and Matsumura, M. (2004). Quantitative analysis of superoxide ion and hydrogen peroxide produced from molecular oxygen on photoirradiated TiO2 particles. J. Cat. *225*, 223–229.

102. Nosaka, Y., and Nosaka, A. (2016). Understanding hydroxyl radical (●OH) generation processes in photocatalysis. ACS Energy Lett *1*, 356–359.

103. Back, S., Tran, K., and Ulissi, Z.W. (2019). Toward a design of active oxygen evolution catalysts: insights from automated density functional theory calculations and machine learning. ACS Catal *9*, 7651–7659.

104. Back, S., Tran, K., and Ulissi, Z.W. (2020). Discovery of acid-stable oxygen evolution catalysts: high-throughput computational screening of equimolar bimetallic oxides. ACS Appl. Mater. Interfaces *12*, 38256–38265.

105. Wenderich, K., Kwak, W., Grimm, A., Kramer, G.J., Mul, G., and Mei, B. (2020). Industrial feasibility of anodic hydrogen peroxide production through photoelectrochemical water splitting: a techno-economic analysis. Sustain. Energy Fuels *4*, 3143–3156.